

- ceptor 2 expression levels and high microvessel density in colorectal cancer. *Oncol Lett.* 2011;2:1101–1106.
31. Lin S, Li H, Mu H, et al. Let-7b regulates the expression of the growth hormone receptor gene in deletion-type dwarf chickens. *BMC Genomics.* 2012;13:306.
 32. Zehavi L, Avraham R, Barzilai A, et al. Silencing of a large microRNA cluster on human chromosome 14q32 in melanoma: biological effects of mir-376a and mir-376c on insulin growth factor 1 receptor. *Mol Cancer.* 2012;11:44.
 33. Noonan EJ, Place RF, Basak S, Pookot D, Li LC. miR-449a causes Rb-dependent cell cycle arrest and senescence in prostate cancer cells. *Oncotarget.* 2010;1:349–358.
 34. Chen H, Lin YW, Mao YQ, et al. MicroRNA-449a acts as a tumor suppressor in human bladder cancer through the regulation of pocket proteins. *Cancer Lett.* 2012;320:40–47.
 35. Jeon HS, Lee SY, Lee EJ, et al. Combining microRNA-449a/b with a HDAC inhibitor has a synergistic effect on growth arrest in lung cancer. *Lung Cancer.* 2012;76:171–176.
 36. John B, Enright AJ, Aravin A, Tuschl T, Sander C, Marks DS. Human MicroRNA targets. *PLoS Biol.* 2004;2:e363.
 37. Hunter MP, Ismail N, Zhang X, et al. Detection of microRNA expression in human peripheral blood microvesicles. *PLoS One.* 2008;3:e3694.
 38. Turchinovich A, Weiz L, Langheinz A, Burwinkel B. Characterization of extracellular circulating microRNA. *Nucleic Acids Res.* 2011;39:7223–7233.
 39. Linsen SE, de Wit E, de Bruijn E, Cuppen E. Small RNA expression and strain specificity in the rat. *BMC Genomics.* 2010;11:249.
 40. Sahoo S, Klychko E, Thorne T, et al. Exosomes from human CD34⁺ stem cells mediate their proangiogenic paracrine activity. *Circ Res.* 2011;109:724–728.



Members have FREE online access to current endocrine
Clinical Practice Guidelines.

www.endo-society.org/guidelines

Overexpression of Leptin Reduces the Ratio of Glycolytic to Oxidative Enzymatic Activities without Changing Muscle Fiber Types in Mouse Skeletal Muscle

Shinya Masuda,^{*,a,†} Tomohiro Tanaka,^{b,‡} Hiroaki Masuzaki,^{b,§} Kazuwa Nakao,^{b,‡} and Sadayoshi Taguchi^{a,§}

^aGraduate School of Human and Environmental Studies, Kyoto University; Yoshida-nihonmatsu-cho, Sakyo-ku, Kyoto 606–8501, Japan; and ^bDepartment of Medicine and Clinical Science, Graduate School of Medicine, Kyoto University; 54 Shogoin-kawahara-cho, Sakyo-ku, Kyoto 606–8507, Japan.

Received July 16, 2013; accepted October 13, 2013

Increased spontaneous locomotive activity and oxygen consumption have been reported in transgenic mice overexpressing leptin in the liver. In the present study, we examined whether the overexpression of leptin altered glycolytic and oxidative metabolic enzymatic activities as well as the composition of myosin heavy chain (MHC) isoforms in skeletal muscle. Enzymatic activities of lactate dehydrogenase (LDH) and citrate synthase (CS) were quantified in gastrocnemius muscle (GAS) and the red portion of tibialis anterior muscle (TA) from leptin transgenic (Tg) mice and non-Tg mice. The composition of MHC isoforms was measured in soleus muscle (SOL) and extensor digitorum longus muscle (EDL) from the two groups. In red TA, LDH-to-CS ratio was significantly lower in Tg than in non-Tg ($p=0.014$), whereas no significant change was observed in GAS. The composition of MHC isoforms was not significantly different in SOL or EDL between Tg and non-Tg groups. Our data indicate that chronic overexpression of leptin reduces the ratio of glycolytic to oxidative capacity without changing muscle fiber types particularly in red muscles. This metabolic change may contribute to the increased spontaneous locomotive activity and oxygen consumption in Tg mice reported previously.

Key words leptin; myosin heavy chain; lactate dehydrogenase; citrate synthase

Leptin is an adipocyte-derived hormone that plays a role in regulating body weight by enhancing energy metabolism and reducing appetite. Transgenic mice that overexpress leptin in the liver¹⁾ and mice chronically treated with leptin²⁾ showed lean phenotype and improved glucose homeostasis. Skeletal muscle is one of the targets of leptin and accounts for about 70–80% of insulin-induced glucose uptake,³⁾ thus skeletal muscle is one of the key organs for glucose homeostasis. Chronic and acute treatment of leptin has been shown to facilitate glucose uptake and fatty acid oxidation *via* activation of AMP-activated protein kinase (AMPK) in skeletal muscle.^{4,5)} These findings support the ongoing efforts for the therapeutic application of leptin for the treatment of insulin resistance and type 2 diabetes,^{6,7)} warranting further research to overcome leptin resistance in diet-induced obesity.^{4,8,9)}

Our group previously showed increased spontaneous locomotive activity and greater oxygen consumption in leptin transgenic mice chronically overexpressing leptin in the liver compared to normal mice.⁴⁾ This finding allows us to postulate that chronic treatment of leptin may enhance the fatigue resistance of skeletal muscle by improving oxidative capacity.

Because AMPK plays a pivotal role in mitochondrial biogenesis in muscle cell,¹⁰⁾ upregulated AMPK activity induced by chronic overexpression of leptin may enhance oxidative capacity more strongly compared to glycolytic capacity in skeletal muscle. In fact, a previous study¹¹⁾ has shown that chronic treatment with 5-aminoimidazole-4-carboxamide-1- β -D-ribofuranoside (AICAR), a cell permeable activator of AMPK, increased metabolic enzymatic activities for mitochondrial respiration and β -oxidation with a decrease in glycolytic enzyme activity. High oxidative capacity relative to glycolytic capacity, a typical metabolic property observed in slow-type muscle fibers¹²⁾ and in endurance-trained skeletal muscles,¹³⁾ confers muscle fibers fatigue-resistant. Enhanced fatigue resistance in skeletal muscle may improve the effectiveness of exercise programs for obesity and metabolic disorders.

In addition to their metabolic properties, muscle fiber types classified by myosin heavy chain (MHC) isoforms are also involved in the fatigue resistance of skeletal muscle. In mammalian limb skeletal muscles, MHC isoforms consist of type I, IIa, IIx, and IIb, and muscle fiber types classified by the four MHC isoforms possess different ATPase activity and tension cost as well as shortening velocity.^{14,15)} Endurance training¹⁶⁾ and chronic muscle contraction¹⁷⁾ change the composition of MHC isoforms, and this change is considered as one of the functional adaptations to improve fatigue resistance in skeletal muscle. However, it is unknown if chronic overexpression of leptin alters muscle fiber types represented by MHC isoforms.

In the present study, we examined the long-term effect of the overexpression of leptin on MHC isoforms and metabolic enzymatic activities in skeletal muscle. For this purpose we used leptin transgenic skinny mice where serum leptin level is five times higher than that of wild-type mice.⁴⁾ The data presented here indicate that chronic overexpression of leptin

The authors declare no conflict of interest.

[†]Present address: Department of Stem Cell Biology, Atomic Bomb Disease Institute, Nagasaki University; 1–12–4 Sakamoto, Nagasaki 852–8523, Japan.

[‡]Present address: Medical Innovation Center, Graduate School of Medicine, Kyoto University; 53 Shogoin-kawahara-cho, Sakyo-ku, Kyoto 606–8507, Japan.

[§]Present address: Second Department of Internal Medicine, Graduate School of Medicine, University of the Ryukyus; 207 Uehara Nishihara, Okinawa 903–0215, Japan.

[§]Present address: Graduate School of Sport and Health Science, Ritsumeikan University; 1–1–1 Noji-higashi, Kusatsu-shi, Shiga 525–8577, Japan.

*To whom correspondence should be addressed. e-mail: smasuda@nagasaki-u.ac.jp

© 2014 The Pharmaceutical Society of Japan

enhance the metabolic capacity for oxidation as opposed to lactate fermentation without changing muscle fiber types in red skeletal muscle.

MATERIALS AND METHODS

Sample Preparation All experimental procedures were undertaken in accordance with the guidelines for animal experiments of Kyoto University and were approved by the Animal Research Committee of Graduate School of Human and Environmental Studies, Kyoto University and by the Animal Research Committee of Graduate School of Medicine, Kyoto University. Leptin transgenic (Tg) mice were prepared as reported previously.¹¹ In this mouse model, a fusion gene comprising the human serum amyloid P component promoter and mouse leptin cDNA coding sequences was inserted to the genomic DNA so that the transgene expression was targeted to the liver. Compared to the leptin transgenic mice to which an adipocyte-specific promoter was applied,¹⁸ our mouse model exhibited higher plasma leptin concentration and showed a skinny phenotype. Male Tg mice ($n=5$) and non-Tg mice ($n=7$) aged 13 or 15 weeks old were housed in temperature-controlled room and fed *ad libitum*. After overnight fasting, the soleus (SOL), extensor digitorum longus (EDL), tibialis anterior (TA), and gastrocnemius (GAS) muscles were dissected from the mice under anesthesia. TA was cut into white and red portions. The dissected muscles were immediately frozen and stored at -80°C . Blood samples were obtained from the abdominal aorta, and blood lactate concentration was immediately measured using Lactate Pro (Arkray, Kyoto, Japan).

MHC Isoforms The composition of MHC isoforms of SOL and EDL was measured as described previously.¹⁹⁻²¹ Briefly, the samples were separated on an SDS-polyacrylamide (7%) gel, and then the gel was stained with coomassie brilliant blue. The bands representing MHCs were classified as type I, IIa/x or IIb isoforms, and the intensity of the bands was quantified using MultiAnalyst software (Bio-Rad, CA, U.S.A.). The composition of MHC isoforms was calculated so that the total percentage of the three isoforms reached 100% in each lane. The percentage of each MHC isoform in Tg groups was statistically compared with the percentage of the corresponding MHC isoform in non-Tg group.

Metabolic Enzyme Activities Activities of lactate dehydrogenase (LDH) and citrate synthase (CS), representative enzymes for glycolytic capacity and mitochondrial respiratory capacity, respectively,²² were measured as described previously.¹⁹ GAS and the red portion of TA were homogenized in homogenate buffer (1:20 w/v). The homogenates were frozen and thawed three times and the supernatants were used for the measurement. Absorbance of the samples was measured for 5 min at 30°C .

Statistical Analysis Data are shown as mean \pm standard error (S.E.). Student's *t*-test was performed to compare between Tg and non-Tg groups. A *p* value of <0.05 was considered statistically significant.

RESULTS

Body weight in Tg and non-Tg groups is shown in Fig. 1. Although the difference in average body weight was not statistically significant, four of five Tg mice showed lower body

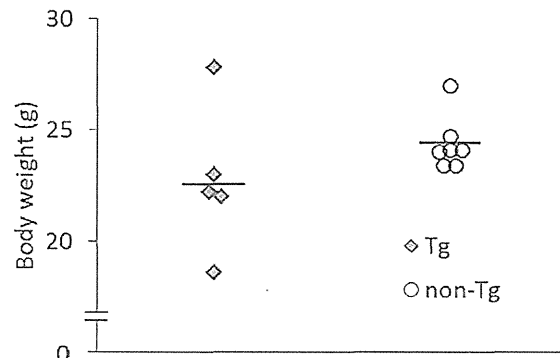


Fig. 1. Body Weight in Tg and Non-Tg Mice

Dots indicate body weight of individual mice in Tg ($n=5$) and non-Tg ($n=7$) groups. Horizontal bars indicate mean value in each group.

Table 1. Blood Lactate Concentration in Tg and Non-Tg Mice

	Tg	Non-Tg
Lactate (mmol/L)	7.9 ± 2.2	8.6 ± 1.8

Values are expressed as mean \pm S.E. ($n=5$ for Tg and $n=7$ for non-Tg).

weight than that of all seven non-Tg mice, indicating that the constitutive expression of leptin contributed to the reduction in body weight. Blood lactate concentration was not significantly different between Tg and non-Tg groups (Table 1).

Enzymatic activities are shown in Fig. 2. LDH activity was not significantly different between Tg and non-Tg groups in red TA or GAS. CS activity was not significantly different between the two groups in either muscle. LDH-to-CS ratio in the red TA was significantly lower in the Tg group than in the non-Tg group ($p=0.014$). Composition of MHC isoforms is shown in Fig. 3. Composition of MHC isoforms was not significantly different between Tg and non-Tg in SOL or EDL.

DISCUSSION

The main finding of the present study is that constitutive overexpression of leptin decreased LDH-to-CS ratio in red TA, but not in GAS. SOL and EDL, representative oxidative red muscle and glycolytic white muscle respectively, were examined for MHC isoform pattern, and there was no statistically significant difference between Tg and non-Tg in those muscles. The ratio of metabolic enzyme activities, *e.g.* LDH-to-CS (lactate fermentation/citric acid cycle), is taken as relative measures of metabolic capacities in skeletal muscle.²³ These results suggest that chronic leptin treatment can enhance oxidative capacity relative to glycolytic capacity in the red skeletal muscle without fiber-type change.

Decreased LDH-to-CS ratio in the Tg group could contribute to the increase in aerobic exercise capacity. In voluntary daily activities, average forces exerted by limb muscles are less than 30% of maximal voluntary force,^{24,25} and oxidative fibers are preferentially recruited at this intensity of exercise.²⁶ Blood lactate concentration was not significantly different between Tg and non-Tg groups, suggesting that neither duration nor intensity of anaerobic exercise differed between the two groups. Taken together, low LDH-to-CS ratio in red muscle from Tg mice could contribute to a higher amount of spontaneous locomotive activity at aerobic exercise intensity

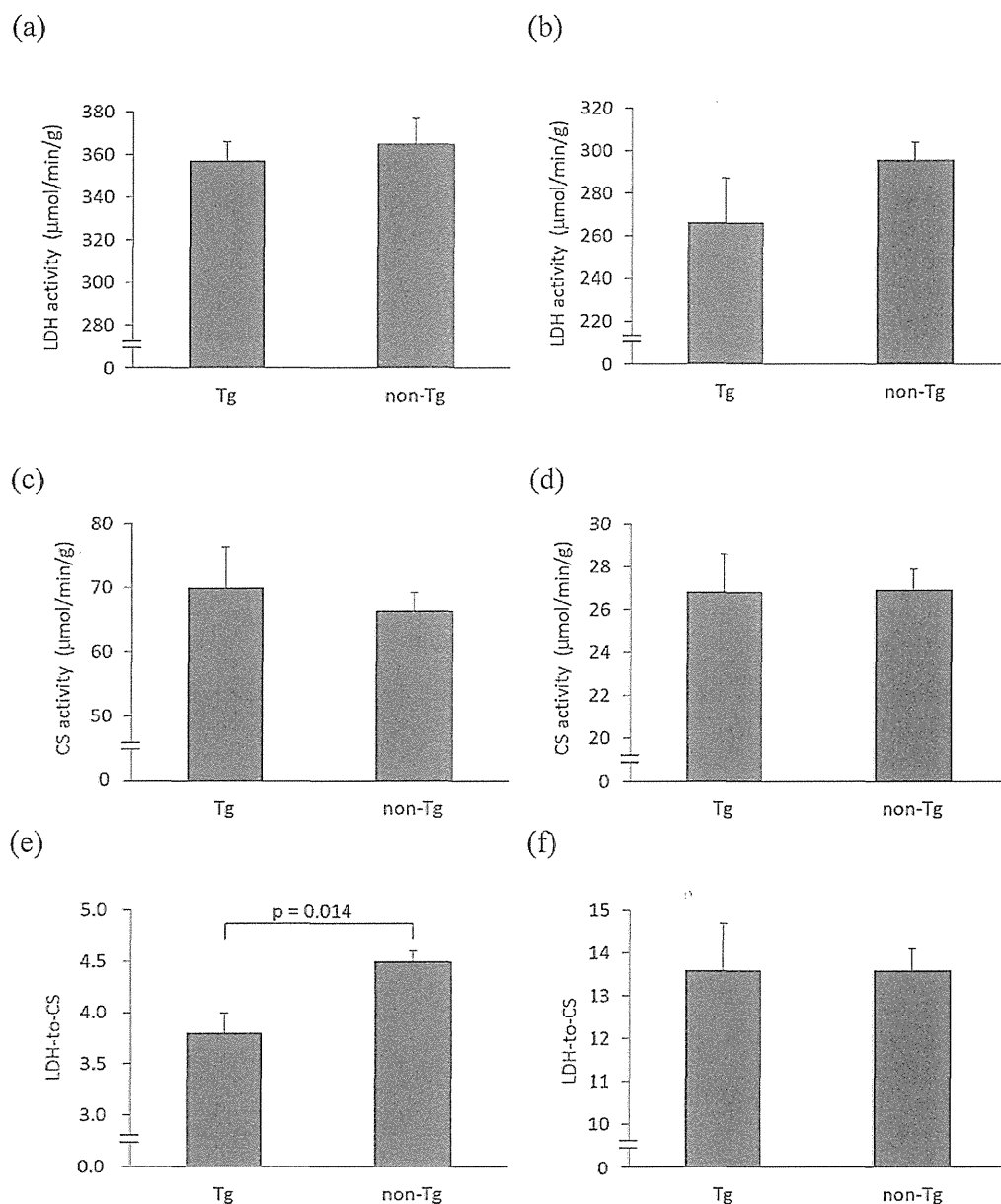


Fig. 2. Metabolic Enzymatic Activities and Ratios in Skeletal Muscle

(a) LDH and (c) CS activities and (e) LDH-to-CS ratio in red TA. (b) LDH and (d) CS activities and (f) LDH-to-CS ratio in GAS. Values are expressed as mean+S.E. ($n=5$ for Tg and $n=7$ for non-Tg).

and thus greater oxygen consumption as reported previously.⁴⁾

Considering our previous study showing elevated phosphorylation level of AMPK α and a high AMP-to-ATP ratio in SOL, a typical red skeletal muscle, from Tg mice,⁴⁾ lower LDH-to-CS ratio observed in red TA from Tg mice could be mediated by increased AMPK activity. Apart from the fact that sympathetic denervation interferes with muscle AMPK activation by leptin,⁵⁾ the precise mechanism for the increased AMPK activity and AMP-to-ATP ratio in red muscle from Tg mice has not been approached. In light of our present data, however, this phenomenon can perhaps be explained by the increased recruitment of oxidative fibers in Tg mice, implied by the increased spontaneous locomotive activity in Tg mice as stated above. A previous study²⁷⁾ showed that the mitochondrial metabolic enzymes such as CS and carni-

tine palmitoyltransferase II had higher activities in skeletal muscles from cp/cp rats, which possess an autosomal recessive mutation in the leptin receptor gene, than in skeletal muscles from homozygous wild-type and heterozygotes. The findings of McClelland *et al.* may argue against our results showing leptin-dependent decrease in LDH-to-CS ratio. Chronic exposure of these rats to leptin may give answers to the question of whether the leptin receptor is necessary for the changes in metabolic enzyme activities in skeletal muscle.

Our results on MHC isoforms suggest that a higher amount of spontaneous locomotive activity or greater oxygen consumption in Tg mice was not attributable to the change in muscle fiber types. Putman *et al.*¹¹⁾ showed that chronic AICAR administration increased CS activity and decreased LDH activity without significant changes in the composition

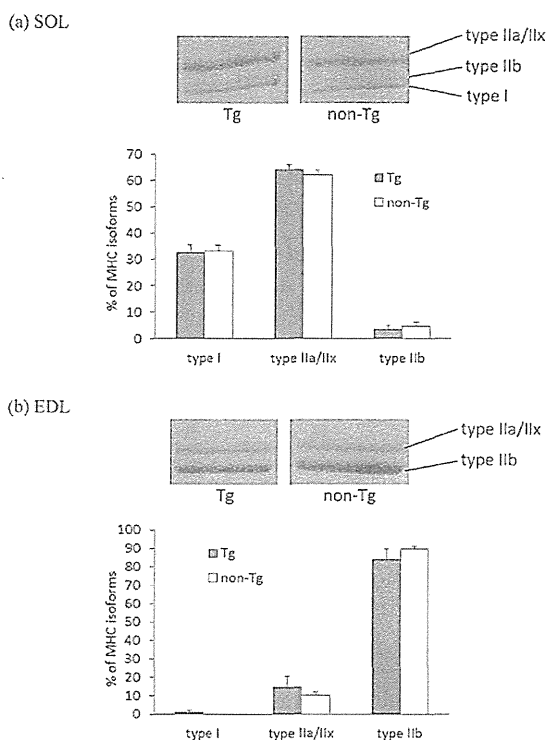


Fig. 3. Composition of MHC Isoforms in Skeletal Muscle

Values are expressed as mean+S.E. ($n=5$ for Tg and $n=7$ for non-Tg). Representative MHC bands are shown above the graphs.

of MHC isoforms or fiber types in rat skeletal muscle, which corresponded to the present study. The effect of leptin on muscle fiber types *via* AMPK may not be as evident as the effect of leptin on metabolic enzyme activities.

In the present study, Tg mice group showed a tendency for lower body weight compared to non-Tg. Our previous study⁴⁾ showed significant reduction in body weight in Tg mice with a similar level of food intake. Therefore, the weight-losing effect by the chronic overexpression of leptin can be attributed primarily to high oxygen consumption and increased spontaneous locomotive activity. Together with our previous data, the present study underscores the importance of chronic leptin treatment as a metabolic modifier that increases oxidative capacity relative to glycolytic capacity in red skeletal muscle.

Some pathological conditions could be observed as a result of constitutively high leptin concentration. For instance, Tg mice exhibited significant elevation in systolic blood pressure and urinary norepinephrine excretion.²⁸⁾ Obesity-induced hyperleptinemia played a crucial role in the progression of non-alcoholic steatohepatitis *via* enhanced responsiveness to endotoxin in the liver.²⁹⁾ Hyperleptinemia in obese people leads to "leptin resistance" as well, under which the anti-obesity effect of leptin is attenuated.³⁰⁾ Therefore, in order to prevent those side effects, the dose and frequency of leptin administration should be properly controlled in clinical applications.

Acknowledgments We are grateful to Miwa Iida, Shin Nohara and Radiance Lim for assistance. We appreciate cooperation by Dr. Tatsuya Hayashi in the present study. This work was supported by MEXT Grants-in-Aid B2:16390267, S2:16109007, B:18790634, B:25282201, and adipomics:15081101; a MHLW Health and Labor Science Re-

search Grant; and Grants from JST, AstraZeneca, the Takeda Medical Research Foundation, the Smoking Research Foundation, Metabolic Syndrome Foundation, the Japan Foundation for Applied Enzymology.

REFERENCES

- Ogawa Y, Masuzaki H, Hosoda K, Aizawa-Abe M, Suga J, Suda M, Ebihara K, Iwai H, Matsuoka N, Satoh N, Odaka H, Kasuga H, Fujisawa Y, Inoue G, Nishimura H, Yoshimasa Y, Nakao K. Increased glucose metabolism and insulin sensitivity in transgenic skinny mice overexpressing leptin. *Diabetes*, **48**, 1822–1829 (1999).
- Kusakabe T, Tanioka H, Ebihara K, Hirata M, Miyamoto L, Miyanaga F, Hige H, Aotani D, Fujisawa T, Masuzaki H, Hosoda K, Nakao K. Beneficial effects of leptin on glycaemic and lipid control in a mouse model of type 2 diabetes with increased adiposity induced by streptozotocin and a high-fat diet. *Diabetologia*, **52**, 675–683 (2009).
- DeFronzo RA, Jacot E, Jequier E, Maeder E, Wahren J, Felber JP. The effect of insulin on the disposal of intravenous glucose. Results from indirect calorimetry and hepatic and femoral venous catheterization. *Diabetes*, **30**, 1000–1007 (1981).
- Tanaka T, Hidaka S, Masuzaki H, Yasue S, Minokoshi Y, Ebihara K, Chusho H, Ogawa Y, Toyoda T, Sato K, Miyanaga F, Fujimoto M, Tomita T, Kusakabe T, Kobayashi N, Tanioka H, Hayashi T, Hosoda K, Yoshimatsu H, Sakata T, Nakao K. Skeletal muscle AMP-activated protein kinase phosphorylation parallels metabolic phenotype in leptin transgenic mice under dietary modification. *Diabetes*, **54**, 2365–2374 (2005).
- Minokoshi Y, Kim YB, Peroni OD, Fryer LG, Muller C, Carling D, Kahn BB. Leptin stimulates fatty-acid oxidation by activating AMP-activated protein kinase. *Nature*, **415**, 339–343 (2002).
- Nakao K, Yasoda A, Ebihara K, Hosoda K, Mukoyama M. Translational research of novel hormones: lessons from animal models and rare human diseases for common human diseases. *J. Mol. Med. (Berl.)*, **87**, 1029–1039 (2009).
- Mantzoros CS, Magkos F, Brinkoetter M, Sienkiewicz E, Dardeno TA, Kim SY, Hamnvik OP, Koniaris A. Leptin in human physiology and pathophysiology. *Am. J. Physiol. Endocrinol. Metab.*, **301**, E567–E584 (2011).
- El-Haschimi K, Pierroz DD, Hileman SM, Bjorbaek C, Flier JS. Two defects contribute to hypothalamic leptin resistance in mice with diet-induced obesity. *J. Clin. Invest.*, **105**, 1827–1832 (2000).
- Tanaka T, Masuzaki H, Yasue S, Ebihara K, Shiuchi T, Ishii T, Arai N, Hirata M, Yamamoto H, Hayashi T, Hosoda K, Minokoshi Y, Nakao K. Central melanocortin signaling restores skeletal muscle AMP-activated protein kinase phosphorylation in mice fed a high-fat diet. *Cell Metab.*, **5**, 395–402 (2007).
- McGee SL, Hargreaves M. AMPK-mediated regulation of transcription in skeletal muscle. *Clin. Sci. (Lond.)*, **118**, 507–518 (2010).
- Putman CT, Kiricsi M, Pearcey J, MacLean IM, Bamford JA, Murdoch GK, Dixon WT, Pette D. AMPK activation increases uncoupling protein-3 expression and mitochondrial enzyme activities in rat muscle without fibre type transitions. *J. Physiol.*, **551**, 169–178 (2003).
- Quiroz-Rothe E, Rivero JL. Coordinated expression of myosin heavy chains, metabolic enzymes, and morphological features of porcine skeletal muscle fiber types. *Microsc. Res. Tech.*, **65**, 43–61 (2004).
- Chi MM, Hintz CS, Coyle EF, Martin WH 3rd, Ivy JL, Nemeth PM, Holloszy JO, Lowry OH. Effects of detraining on enzymes of energy metabolism in individual human muscle fibers. *Am. J. Physiol.*, **244**, C276–C287 (1983).
- Bottinelli R, Canepari M, Reggiani C, Stienen GJ. Myofibrillar ATPase activity during isometric contraction and isomyosin composition in rat single skinned muscle fibres. *J. Physiol.*, **481**, 663–675

- (1994).
- 15) Schiaffino S, Reggiani C. Fiber types in mammalian skeletal muscles. *Physiol. Rev.*, **91**, 1447–1531 (2011).
 - 16) Sullivan VK, Powers SK, Criswell DS, Turner N, Larochele JS, Lowenthal D. Myosin heavy chain composition in young and old rat skeletal muscle: effects of endurance exercise. *J. Appl. Physiol.*, **78**, 2115–2120 (1995).
 - 17) Termin A, Staron RS, Pette D. Changes in myosin heavy chain isoforms during chronic low-frequency stimulation of rat fast hindlimb muscles. A single-fiber study. *Eur. J. Biochem.*, **186**, 749–754 (1989).
 - 18) Ioffe E, Moon B, Connolly E, Friedman JM. Abnormal regulation of the leptin gene in the pathogenesis of obesity. *Proc. Natl. Acad. Sci. U.S.A.*, **95**, 11852–11857 (1998).
 - 19) Masuda S, Hayashi T, Egawa T, Taguchi S. Evidence for differential regulation of lactate metabolic properties in aged and unloaded rat skeletal muscle. *Exp. Gerontol.*, **44**, 280–288 (2009).
 - 20) Miyazaki M, Hitomi Y, Kizaki T, Ohno H, Haga S, Takemasa T. Contribution of the calcineurin signaling pathway to overload-induced skeletal muscle fiber-type transition. *J. Physiol. Pharmacol.*, **55**, 751–764 (2004).
 - 21) Talmadge RJ, Roy RR. Electrophoretic separation of rat skeletal muscle myosin heavy-chain isoforms. *J. Appl. Physiol.*, **75**, 2337–2340 (1993).
 - 22) Powers SK, Lawler J, Criswell D, Lieu FK, Dodd S. Alterations in diaphragmatic oxidative and antioxidant enzymes in the senescent Fischer 344 rat. *J. Appl. Physiol.*, **72**, 2317–2321 (1992).
 - 23) Bass A, Brdiczka D, Eyer P, Hofer S, Pette D. Metabolic differentiation of distinct muscle types at the level of enzymatic organization. *Eur. J. Biochem.*, **10**, 198–206 (1969).
 - 24) Kern DS, Semmler JG, Enoka RM. Long-term activity in upper- and lower-limb muscles of humans. *J. Appl. Physiol.*, **91**, 2224–2232 (2001).
 - 25) Shirasawa H, Kanehisa H, Kouzaki M, Masani K, Fukunaga T. Differences among lower leg muscles in long-term activity during ambulatory condition without any moderate to high intensity exercise. *J. Electromyogr. Kinesiol.*, **19**, e50–e56 (2009).
 - 26) Sale DG. Influence of exercise and training on motor unit activation. *Exerc. Sport Sci. Rev.*, **15**, 95–151 (1987).
 - 27) McClelland GB, Kraft CS, Michaud D, Russell JC, Mueller CR, Moyes CD. Leptin and the control of respiratory gene expression in muscle. *Biochim. Biophys. Acta*, **1688**, 86–93 (2004).
 - 28) Aizawa-Abe M, Ogawa Y, Masuzaki H, Ebihara K, Satoh N, Iwai H, Matsuoka N, Hayashi T, Hosoda K, Inoue G, Yoshimasa Y, Nakao K. Pathophysiological role of leptin in obesity-related hypertension. *J. Clin. Invest.*, **105**, 1243–1252 (2000).
 - 29) Imajo K, Fujita K, Yoneda M, Nozaki Y, Ogawa Y, Shinohara Y, Kato S, Mawatari H, Shibata W, Kitani H, Ikejima K, Kirikoshi H, Nakajima N, Saito S, Maeyama S, Watanabe S, Wada K, Nakajima A. Hyperresponsivity to low-dose endotoxin during progression to nonalcoholic steatohepatitis is regulated by leptin-mediated signaling. *Cell Metab.*, **16**, 44–54 (2012).
 - 30) Könnner AC, Brüning JC. Selective insulin and leptin resistance in metabolic disorders. *Cell Metab.*, **16**, 144–152 (2012).

Intracerebroventricular Administration of C-Type Natriuretic Peptide Suppresses Food Intake via Activation of the Melanocortin System in Mice

Nobuko Yamada-Goto,¹ Goro Katsuura,¹ Ken Ebihara,¹ Megumi Inuzuka,¹ Yukari Ochi,¹ Yui Yamashita,¹ Toru Kusakabe,¹ Akihiro Yasoda,¹ Noriko Satoh-Asahara,² Hiroyuki Ariyasu,¹ Kiminori Hosoda,¹ and Kazuwa Nakao¹

C-type natriuretic peptide (CNP) and its receptor are abundantly distributed in the brain, especially in the arcuate nucleus (ARC) of the hypothalamus associated with regulating energy homeostasis. To elucidate the possible involvement of CNP in energy regulation, we examined the effects of intracerebroventricular administration of CNP on food intake in mice. The intracerebroventricular administration of CNP-22 and CNP-53 significantly suppressed food intake on 4-h refeeding after 48-h fasting. Next, intracerebroventricular administration of CNP-22 and CNP-53 significantly decreased nocturnal food intake. The increment of food intake induced by neuropeptide Y and ghrelin was markedly suppressed by intracerebroventricular administration of CNP-22 and CNP-53. When SHU9119, an antagonist for melanocortin-3 and melanocortin-4 receptors, was coadministered with CNP-53, the suppressive effect of CNP-53 on refeeding after 48-h fasting was significantly attenuated by SHU9119. Immunohistochemical analysis revealed that intracerebroventricular administration of CNP-53 markedly increased the number of c-Fos-positive cells in the ARC, paraventricular nucleus, dorsomedial hypothalamus, ventromedial hypothalamic nucleus, and lateral hypothalamus. In particular, c-Fos-positive cells in the ARC after intracerebroventricular administration of CNP-53 were coexpressed with α -melanocyte-stimulating hormone immunoreactivity. These results indicated that intracerebroventricular administration of CNP induces an anorexigenic action, in part, via activation of the melanocortin system. *Diabetes* 62:1500–1504, 2013

C-type natriuretic peptide (CNP) is a member of the natriuretic peptide family and has been demonstrated to be abundantly present in the brain, interestingly in discrete hypothalamic areas, such as the arcuate nucleus (ARC) of the hypothalamus, that play pivotal roles in energy regulation (1–3). Two predominant molecular forms of CNP in the porcine brain were reported to be a 22-residue peptide (CNP-22) and its N-terminally elongated 53-residue peptide (CNP-53) (1). Moreover, natriuretic peptide receptor-B (NPR-B), a CNP receptor, is also widely distributed in the brain and is reported to be abundantly expressed in the ARC of the

hypothalamus (4,5). These findings indicate the possibility that the brain CNP/NPR-B system may regulate energy homeostasis.

In the current study, we examined the effects of intracerebroventricular administration of CNP on food intake induced by refeeding after fasting and by orexigenic peptides, such as neuropeptide Y (NPY) and ghrelin. Also, we examined the involvement of the melanocortin system in the CNP actions.

RESEARCH DESIGN AND METHODS

Animals and diets. Male C57BL/6J mice (6 weeks old) obtained from Japan SLC (Shizuoka, Japan) were housed in plastic cages in a room kept at a room temperature of $23 \pm 1^\circ\text{C}$ and a 12:12-h light–dark cycle (lights turned on at 9:00 A.M.). The mice had ad libitum access to water and food (CE-2; CLEA Japan, Tokyo, Japan). All experiments were performed at 10 weeks of age in accordance with the guidelines established by the Institutional Animal Investigation Committee at Kyoto University and the United States National Institutes of Health Guide for the Care and Use of Laboratory Animals. Every effort was made to optimize comfort and to minimize the use of animals.

Peptides. CNP-22, CNP-53, ghrelin, and NPY were purchased from Peptide Institute (Osaka, Japan). SHU9119 was purchased from Bachem AG (Bubendorf, Switzerland).

Intracerebroventricular injection. Intracerebroventricular injection was performed according to our previous report (6).

Measurement of food intake

Fasting-refeeding. Mice were fasted for 48 h and then refed for 4 h. Water was available ad libitum during the experiments. The intracerebroventricular or intraperitoneal administration of CNP-22 or CNP-53 was performed just before refeeding. Food intake was measured for 4 h of refeeding. At the end of experiments, the hypothalamus was collected for examination of the expressions of mRNA for neuropeptides (7).

Nocturnal food intake. To assess the effect of intracerebroventricular administration of CNP-22 or CNP-53 on nocturnal food intake, peptides were injected intracerebroventricularly 1 h before the beginning of the dark phase. Food intake was measured for 15 h after intracerebroventricular injection. Water was available ad libitum during the experiments.

Food intake induced by NPY and ghrelin. The experiments were performed from 11:00 A.M. to 3:00 P.M. CNP-22 or CNP-53 was intracerebroventricularly administered just before intracerebroventricular injection of NPY (5 nmol/mouse) or intraperitoneal injection of ghrelin (100 nmol/kg). Food intake was measured for 4 h after peptide injection. In these experiments, food and water were available ad libitum.

PCR. The extraction of mRNA and quantitative real-time RT-PCR were performed according to our previous report (8). Primers for prepro-melanocortin, cocaine and amphetamine-related peptide, NPY, agouti gene-related peptide (AgRP) and glyceraldehyde 3-phosphate dehydrogenase are shown in Supplementary Table 1.

Immunohistochemistry for c-Fos and α -MSH in the hypothalamus. The immunohistochemical methods and the stereotaxic coordinates for the hypothalamic nuclei were based on our previous report (6). Briefly, mice were anesthetized with pentobarbital at 1 h after intracerebroventricular injection of CNP-53 (1.5 nmol/mouse) and perfused with 50 mL 0.1 mol/L PBS, followed by 50 mL ice-cold 4% paraformaldehyde in 0.1 mol/L PBS. Sections of 30- μm thickness were cut with a cryostat. According to the mouse brain atlas (9), cross-sections were selected in correspondence to -1.70 mm [ARC, lateral hypothalamus (LH), dorsomedial hypothalamus (DMH), ventromedial hypothalamic

From the ¹Department of Medicine and Clinical Science, Kyoto University Graduate School of Medicine, Kyoto, Japan; and the ²Clinical Research Institute, National Hospital Organization, Kyoto Medical Center, Kyoto, Japan. Corresponding author: Nobuko Yamada-Goto, nobukito@kuhp.kyoto-u.ac.jp. Received 31 May 2012 and accepted 7 November 2012. DOI: 10.2337/db12-0718

This article contains Supplementary Data online at <http://diabetes.diabetesjournals.org/lookup/suppl/doi:10.2337/db12-0718/-/DC1>.

© 2013 by the American Diabetes Association. Readers may use this article as long as the work is properly cited, the use is educational and not for profit, and the work is not altered. See <http://creativecommons.org/licenses/by-nc-nd/3.0/> for details.

See accompanying commentary, p. 1379.

nucleus (VMH]) and to -0.82 mm [paraventricular nucleus (PVN)], relative to bregma. For c-Fos and α -melanocyte-stimulating hormone (α -MSH) protein staining, the sections were incubated with anti-c-Fos rabbit antibody (Ab-5; 1:5,000; Oncogene Science, Cambridge, MA) and anti- α -MSH sheep antibody (AB5087; 1:10,000; EMD Millipore, Billerica, MA), respectively. The antibody was detected using the Vectastain ABC Elite kit (PK-6101; Vector Laboratories, Burlingame, CA) and a diaminobenzidine substrate kit (SK-4100; Vector Laboratories) was used for visualization. The second antibodies for fluorescence visualization used were goat anti-rabbit488 (A11008; 1:200; Life Technologies, Carlsbad, CA) for anti-c-Fos rabbit antibody and goat anti-sheep546 (A21098; 1:200; Life Technologies) for anti- α -MSH sheep antibody.

Data analysis. All values are given as the mean \pm SEM. Statistical analysis of the data were performed by ANOVA, followed by the Tukey-Kramer test. Statistical significance was defined as $P < 0.05$.

RESULTS

Effects of intracerebroventricular administration of CNP-22 and CNP-53 on food intake at refeeding after fasting. The intracerebroventricular administration of CNP-22 (1.5 and 4.5 nmol/mouse) and CNP-53 (1.5 nmol/mouse) significantly suppressed food intake during 4-h refeeding after 48-h fasting in comparison with data from saline-treated mice (Fig. 1A). In this experiment, CNP-53 (1.5 nmol), but not other treatments, induced significant reduction of body weight compared with saline treatment (Supplementary Table 2). The mRNA expressions of prepro-melanocortin and cocaine and amphetamine-related peptide significantly decreased, and the mRNA expressions of *NPY* and *AgRP* significantly increased after refeeding compared with control animals (Supplementary Fig. 1). The intracerebroventricular administration of CNP-53 did not influence the mRNA expressions of these neuropeptides in the hypothalamus (Supplementary Fig. 1). Next, the peripheral action of CNP on food intake was examined when a 10-fold greater dose than intracerebroventricular injection of each CNP was intraperitoneally administered. The intraperitoneal administrations of CNP-22 (1.5 μ mol/kg) and CNP-53 (0.5 μ mol/kg) did not change the food intake during 4-h refeeding after 48-h fasting (Fig. 1B), nor were there changes in body weight (Supplementary Table 3).

The intracerebroventricular administrations of CNP-22 (4.5 nmol/mouse) and CNP-53 (1.5 nmol/mouse) at 1 h before the start of the dark phase significantly suppressed nocturnal food intake compared with saline treatment (Fig. 1C).

Effect of intracerebroventricular administration of CNP-22 and CNP-53 on NPY-induced and ghrelin-induced food intake. When CNP-22 (4.5 nmol/mouse) and CNP-53 (1.5 nmol/mouse) were concomitantly administered intracerebroventricularly with NPY, they significantly suppressed the food intake induced by NPY compared with that of saline treatment (Fig. 2A). When CNP-22 (4.5 nmol/mouse) and CNP-53 (1.5 nmol/mouse) were administered intracerebroventricularly with ghrelin, they significantly suppressed the food intake induced by ghrelin compared with that of saline treatment (Fig. 2B).

Effect of melanocortin receptor antagonist, SHU9119, on the anorectic effect of CNP. To examine its involvement in the anorectic effect of CNP, SHU9119 was administered intracerebroventricularly together with CNP-53 (1.5 nmol/mouse). SHU9119 (1 nmol/mouse) significantly attenuated the suppressive action of CNP-53 on the food intake during 4-h refeeding after 48-h fasting, whereas SHU9119 itself significantly enhanced the increase of food intake in comparison with mice administered saline treatment (Fig. 3).

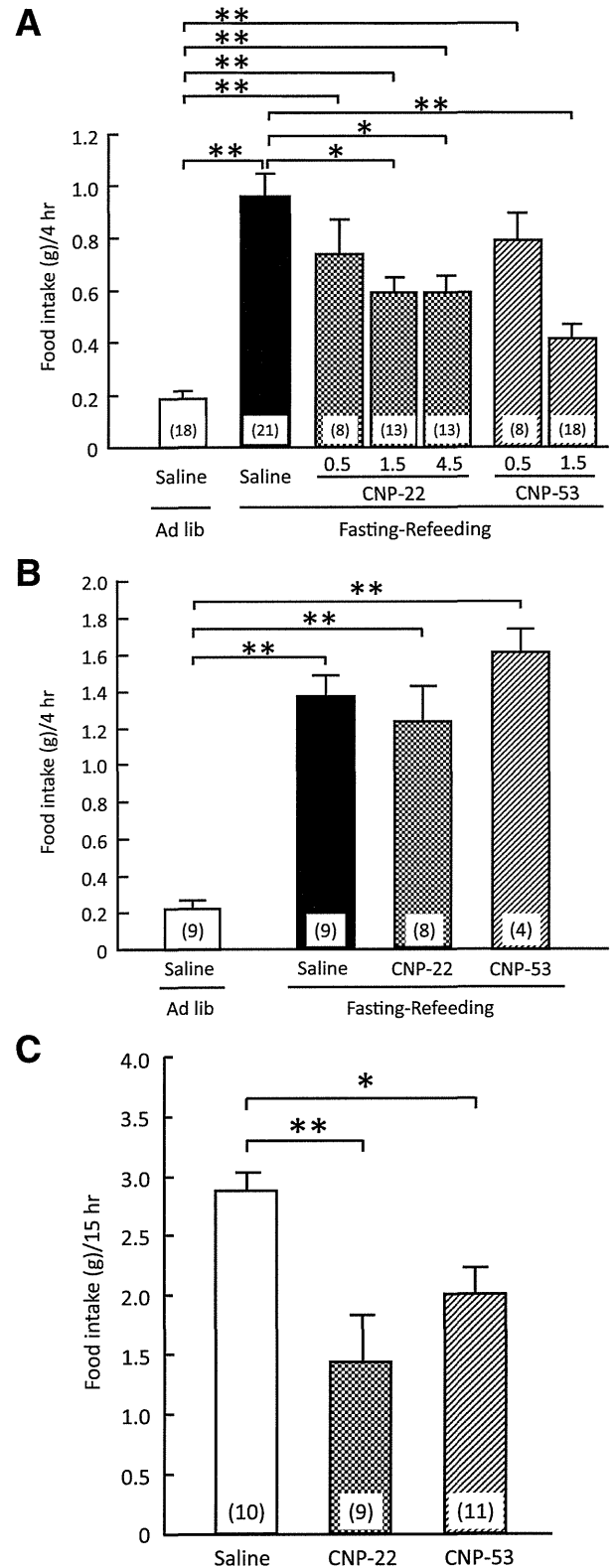


FIG. 1. Effects of CNP on refeeding after fasting. **A:** Effects of intracerebroventricular administration of CNP-22 (0.5, 1.5, and 4.5 nmol/mouse) and CNP-53 (0.5 and 1.5 nmol/mouse) on 4-h refeeding after 48-h fasting in mice. Food intake was observed for 4 h after refeeding. **B:** Effects of intraperitoneal administration of CNP-22 (1.5 μ mol/kg) and CNP-53 (0.5 μ mol/kg) on 4-h refeeding after 48-h fasting in mice. Food intake was observed for 4 h after refeeding. **C:** Effects of intracerebroventricular administration of CNP-22 (4.5 nmol/mouse) and CNP-53 (1.5 nmol/mouse) on nocturnal food intake in mice. Food intake was observed for 15 h after intracerebroventricular injection. Data represent mean \pm SEM. The number of mice is given in parentheses. Significant differences: * $P < 0.05$, ** $P < 0.01$.

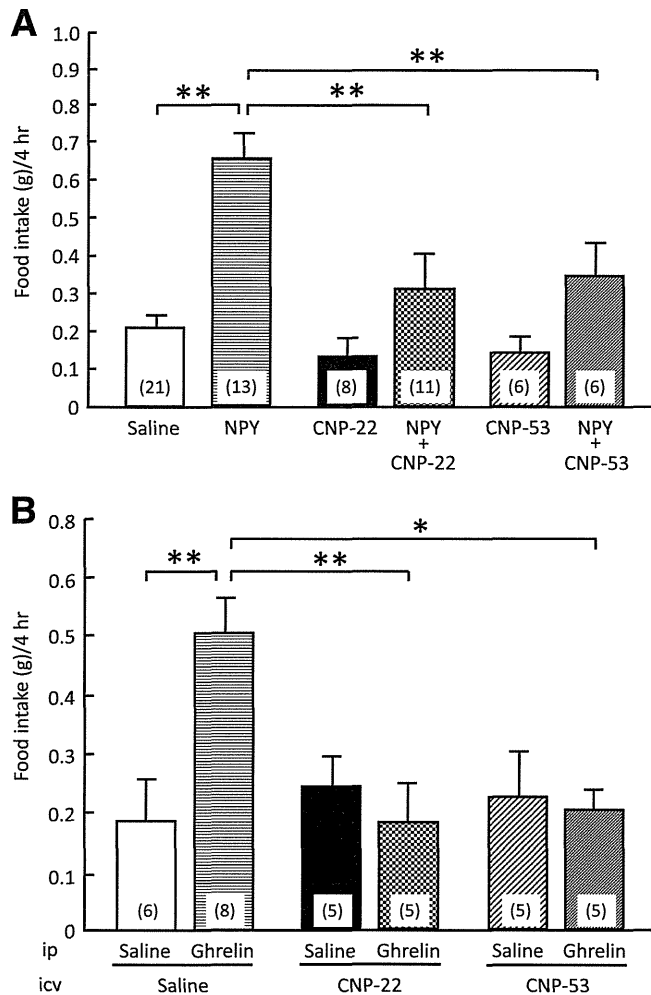


FIG. 2. Effects of CNP-22 and CNP-53 on food intake induced by NPY and ghrelin. **A:** Effects of intracerebroventricular administration of CNP-22 (4.5 nmol/mouse) and CNP-53 (1.5 nmol/mouse) on NPY-induced (5 nmol/mouse, intracerebroventricular) food intake in mice. Food intake was observed for 4 h after coadministration of NPY and CNP. **B:** Effects of intracerebroventricular administration of CNP-22 (4.5 nmol/mouse) and CNP-53 (1.5 nmol/mouse) on ghrelin-induced (100 nmol/kg, intraperitoneal) food intake in mice. Food intake was observed for 4 h after coadministration of ghrelin and CNP. Data represent mean \pm SEM. The number of mice is given in parentheses. Significant differences: * P < 0.05, ** P < 0.01.

c-Fos-immunoreactive cells in the hypothalamus after intracerebroventricular administration of CNP. To understand the neuronal pathway involved in the anorectic actions of CNP, the expression of c-Fos, one of the markers of neuronal activation, was monitored by immunohistochemical examination at 1 h after intracerebroventricular injection of CNP-53 (1.5 nmol/mouse). The numbers of c-Fos-immunoreactive cells in the ARC, PVN, and DMH were predominantly increased after intracerebroventricular injection of CNP-53 in comparison with saline treatment (Fig. 4A). The c-Fos-positive cells were also moderately increased in the VMH and LH (Fig. 4A). Next, we examined whether c-Fos immunoreactivity coexisted with α -MSH-containing cells. In the ARC of saline-treated mice, only a few α -MSH-immunoreactive cells showed weak c-Fos immunoreactivity (Fig. 4B). However, c-Fos-immunoreactive cells that increased with intracerebroventricular administration of CNP-53 in the ARC expressed a large amount of α -MSH immunoreactivity (Fig. 4B).

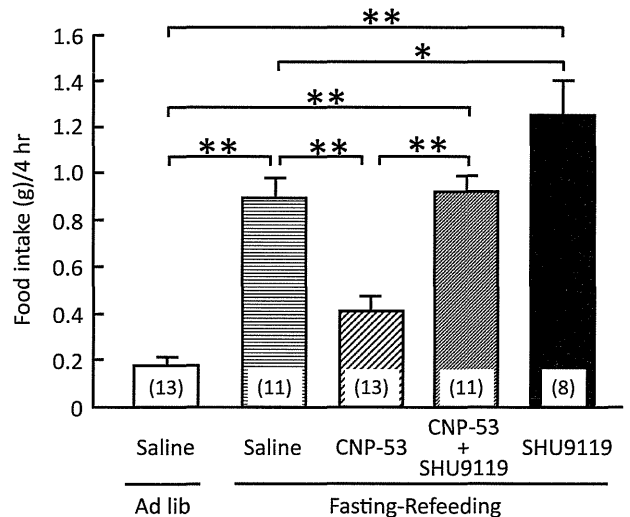


FIG. 3. Effects of intracerebroventricular administration of CNP-53 (1.5 nmol/mouse) and SHU9119 (1 nmol/mouse) on refeeding after 48-h fasting in mice. Food intake was observed for 4 h after refeeding. Data represent mean \pm SEM. The number of mice is given in parentheses. Significant differences: * P < 0.05, ** P < 0.01.

DISCUSSION

The current study demonstrated that intracerebroventricular administration of CNP-22 and CNP-53, but not intraperitoneal injection, led to significant reduction of food intake induced by fasting-refeeding. This reduction was inhibited by the melanocortin-3 receptor (MC3R)/melanocortin-4 receptor (MC4R) antagonist SHU9119. In addition, CNP significantly suppressed nocturnal food intake and orexigenic actions induced by NPY and ghrelin. The immunohistochemical study revealed that intracerebroventricular administration of CNP-53 increased the number of c-Fos-expressing cells containing α -MSH in the hypothalamus. These findings indicated that the intracerebroventricular administration of CNP exhibits anorectic actions partially via activation of the melanocortin system, although the doses of CNP used in the current study could be pharmacological doses.

The hypothalamus is considered to be an important region in regulating energy homeostasis. In particular, the ARC in the hypothalamus contains both an orexigenic peptide, NPY, and an anorectic peptide, α -MSH, and is postulated to be involved in the first-order regulation of food intake. Synthetic MC3R/MC4R agonists, melanotan II, and [Nle⁴-D-Phe⁷]- α -MSH completely blocked food deprivation-induced increase in food intake as well as the food intake stimulated by intracerebroventricular administration of NPY (10,11). Regarding the reciprocal interactions of α -MSH and NPY, melanocortin neurons in the ARC project to the PVN (12). In the current study, intracerebroventricular administration of CNP significantly suppressed food intake after fasting, which was antagonized by SHU9119. Our results also showed that CNP suppressed NPY-induced food intake. Taken together, these findings indicate that CNP exhibits anorectic actions via activation of MC3R/MC4R downstream signaling. However, mRNA expressions of prepro-melanocortin, cocaine and amphetamine-related peptide, NPY, and AgRP in the hypothalamus after the intracerebroventricular injection of CNP-53 in fasting-refeeding experiment did not change compared with those after saline. The reason for this

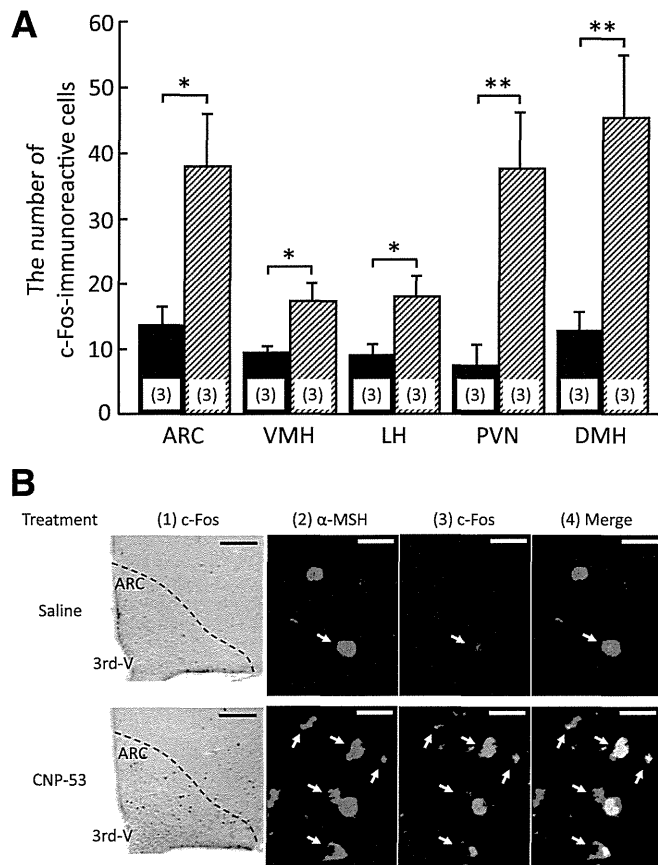


FIG. 4. The c-Fos-immunoreactive cells in the hypothalamus after intracerebroventricular administration of CNP-53 (1.5 nmol/mouse). **A:** Number of c-Fos-immunoreactive cells after saline and CNP-53 treatments. Data represent mean \pm SEM. The number of mice is given in parentheses. Significant differences: * $P < 0.05$, ** $P < 0.01$. **B:** c-Fos-immunoreactive cells induced by intracerebroventricular administration of saline and CNP-53 (1). 3rd-V, the third ventricular. Scale bars, 100 μ m. Coexistence of α -MSH (red) and c-Fos (green) immunoreactivity in the ARC (2–4) after saline (upper) and CNP-53 (1.5 nmol/mouse; lower) treatments. White arrows indicate cells expressing both α -MSH and c-Fos immunoreactivity. 3rd-V, the third ventricular. Scale bars, 20 μ m.

discrepancy may lie in the experimental condition, time course, and regional specificity. To clarify this discrepancy, further examinations will be required.

This study demonstrated that the intracerebroventricular administration of CNP significantly suppressed the nocturnal food intake. Robust feeding during the nocturnal phase of the daily light–dark cycle was demonstrated to be attributed to the upregulation of NPY and its receptors (13). These findings indicate that CNP may decrease food intake in the nocturnal phase via suppression of NPY action.

In the current study, CNP significantly suppressed the increase in food intake induced by ghrelin, an orexigenic hormone secreted by the stomach (14). NPR-B, a CNP receptor, has been identified in appetite-regulating regions, such as the ARC, VMH, PVN, DMH, and LH (15). The systemic administration of ghrelin significantly increased NPY and AgRP expression in the ARC of the hypothalamus in fed and fasted rats (15), resulting in hyperphagia. The intracerebroventricular injection of melanotan II caused a significant decrease in ghrelin-induced food intake (16). These findings suggest that the actions of ghrelin are modulated by α -MSH and NPY systems. Furthermore, plasma ghrelin and hypothalamic ghrelin receptor mRNA

expression are reported to be increased after fasting (17,18). These findings suggest the possibility that intracerebroventricular administration of CNP activates the melanocortin system, which subsequently inhibits the action of NPY, resulting in a reduced increase of food intake induced by ghrelin.

To assess which hypothalamic nucleus is involved in the anorexigenic action of CNP, a marker for neuronal activity, c-Fos expression in the hypothalamus was examined after intracerebroventricular administration of CNP-53. The intracerebroventricular administration of CNP-53 significantly increased the number of c-Fos-expressing cells in several hypothalamic nuclei, such as ARC, PVN, DMH, VMH, and LH, indicating that CNP-53 directly or indirectly stimulates neurons in these hypothalamic nuclei. Especially in the ARC, the result was an increased number of c-Fos-immunoreactive cells containing α -MSH immunoreactivity, indicating that CNP stimulates α -MSH-containing neurons. This possibility is supported by the finding that the suppressive action of CNP-53 on food intake was blocked by concomitant administration of SHU9119, an MC3R/MC4R antagonist.

The current study has demonstrated the anorexigenic action of intracerebroventricular administration of CNP via activation of the melanocortin system. To define the precise effect of CNP in the brain on food intake, further investigation using mice with inducible brain-specific deletion of CNP or NPR-B/NPR-C will be required.

From the present findings, we postulate the possible mechanism for anorexigenic action of exogenous CNP to be as follows: CNP directly or indirectly acts on α -MSH-containing neurons and subsequently stimulates α -MSH release, resulting in suppression of food intake induced by NPY and ghrelin. This possible mechanism may apply to the suppressive effects of CNP on food intake after fasting and in the nocturnal phase. Further work is needed to define the pathophysiological significance of brain CNP in regulation of food intake.

ACKNOWLEDGMENTS

This work was supported in part by research grants from the Ministry of Education, Culture, Sports, Science, and Technology of Japan, and the Ministry of Health, Labour, and Welfare of Japan.

No potential conflicts of interest relevant to this article were reported.

N.Y.-G. and G.K. performed experiments, contributed to discussion, and wrote the manuscript. K.E., M.I., Y.O., Y.Y., T.K., A.Y., N.S.-A., H.A., and K.H. contributed to discussion. K.N. contributed to discussion, and reviewed and edited the manuscript. K.N. is the guarantor of this work and, as such, had full access to all the data in the study and takes responsibility for the integrity of the data and the accuracy of the data analysis.

REFERENCES

- Minamino N, Makino Y, Tateyama H, Kangawa K, Matsuo H. Characterization of immunoreactive human C-type natriuretic peptide in brain and heart. *Biochem Biophys Res Commun* 1991;179:535–542
- Herman JP, Langub MC Jr, Watson RE Jr. Localization of C-type natriuretic peptide mRNA in rat hypothalamus. *Endocrinology* 1993;133:1903–1906
- Langub MC Jr, Watson RE Jr, Herman JP. Distribution of natriuretic peptide precursor mRNAs in the rat brain. *J Comp Neurol* 1995;356:183–199
- Langub MC Jr, Dolgas CM, Watson RE Jr, Herman JP. The C-type natriuretic peptide receptor is the predominant natriuretic peptide receptor mRNA expressed in rat hypothalamus. *J Neuroendocrinol* 1995;7:305–309

5. Herman JP, Dolgas CM, Rucker D, Langub MC Jr. Localization of natriuretic peptide-activated guanylate cyclase mRNAs in the rat brain. *J Comp Neurol* 1996;369:165-187
6. Yamada N, Katsuura G, Ochi Y, Ebihara K, Kusakabe T, Hosoda K, Nakao K. Impaired CNS leptin action is implicated in depression associated with obesity. *Endocrinology* 2011;152:2634-2643
7. Nakao K, Katsuura G, Morii N, Itoh H, Shiono S, Yamada T, Sugawara A, Sakamoto M, Saito Y, Eigyo M, Matsushita A, Imura H. Inhibitory effect of centrally administered atrial natriuretic polypeptide on the brain dopaminergic system in rats. *Eur J Pharmacol* 1986;131:171-177
8. Yamada N, Katsuura G, Tatsuno I, et al. Orexin decreases mRNA expressions of NMDA and AMPA receptor subunits in rat primary neuron cultures. *Peptides* 2008;29:1582-1587
9. Paxinos G, Franklin KBJ. *The mouse brain in stereotaxic coordinates*. New York, Academic Press, 2004
10. Brown KS, Gentry RM, Rowland NE. Central injection in rats of alpha-melanocyte-stimulating hormone analog: effects on food intake and brain Fos. *Regul Pept* 1998;78:89-94
11. Murphy B, Nunes CN, Ronan JJ, et al. Melanocortin mediated inhibition of feeding behavior in rats. *Neuropeptides* 1998;32:491-497
12. Sánchez E, Singru PS, Acharya R, et al. Differential effects of refeeding on melanocortin-responsive neurons in the hypothalamic paraventricular nucleus. *Endocrinology* 2008;149:4329-4335
13. Kalra PS, Dube MG, Xu B, Farmerie WG, Kalra SP. Evidence that dark-phase hyperphagia induced by neurotoxin 6-hydroxydopamine may be due to decreased leptin and increased neuropeptide Y signaling. *Physiol Behav* 1998;63:829-835
14. Kojima M, Hosoda H, Date Y, Nakazato M, Matsuo H, Kangawa K. Ghrelin is a growth-hormone-releasing acylated peptide from stomach. *Nature* 1999;402:656-660
15. Harrold JA, Dovey T, Cai XJ, Halford JC, Pinkney J. Autoradiographic analysis of ghrelin receptors in the rat hypothalamus. *Brain Res* 2008;1196:59-64
16. Shrestha YB, Wickwire K, Giraudo SQ. Action of MT-II on ghrelin-induced feeding in the paraventricular nucleus of the hypothalamus. *Neuroreport* 2004;15:1365-1367
17. Keen-Rhinehart E, Bartness TJ. NPY Y1 receptor is involved in ghrelin- and fasting-induced increases in foraging, food hoarding, and food intake. *Am J Physiol Regul Integr Comp Physiol* 2007;292:R1728-R1737
18. Kim MS, Yoon CY, Park KH, et al. Changes in ghrelin and ghrelin receptor expression according to feeding status. *Neuroreport* 2003;14:1317-1320

Generation of leptin-deficient *Lep^{mkyo}/Lep^{mkyo}* rats and identification of leptin-responsive genes in the liver

Megumi Aizawa-Abe,^{1,2} Ken Ebihara,^{1,2} Chihiro Ebihara,² Tomoji Mashimo,³ Akiko Takizawa,³ Tsutomu Tomita,² Toru Kusakabe,² Yuji Yamamoto,² Daisuke Aotani,^{1,2} Sachiko Yamamoto-Kataoka,² Takeru Sakai,² Kiminori Hosoda,^{1,2,4} Tadao Serikawa,³ and Kazuwa Nakao²

¹Department of Experimental Therapeutics, Translational Research Center, Kyoto University Hospital, Kyoto, Japan;

²Department of Medicine and Clinical Science, Kyoto University Graduate School of Medicine, Kyoto, Japan; ³Institute of Laboratory Animals, Kyoto University Graduate School of Medicine, Kyoto, Japan; and ⁴Department of Health and Science, Kyoto University Graduate School of Medicine, Kyoto, Japan

Submitted 8 March 2013; accepted in final form 24 June 2013

Aizawa-Abe M, Ebihara K, Ebihara C, Mashimo T, Takizawa A, Tomita T, Kusakabe T, Yamamoto Y, Aotani D, Yamamoto-Kataoka S, Sakai T, Hosoda K, Serikawa T, Nakao K. Generation of leptin-deficient *Lep^{mkyo}/Lep^{mkyo}* rats and identification of leptin-responsive genes in the liver. *Physiol Genomics* 45: 786–793, 2013. First published June 25, 2013; doi:10.1152/physiolgenomics.00040.2013.—Leptin is one of the key molecules in maintaining energy homeostasis. Although genetically leptin-deficient *Lep^{ob}/Lep^{ob}* mice have greatly contributed to elucidating leptin physiology, the use of more than one species can improve the accuracy of analysis results. Using the *N*-ethyl-*N*-nitrosourea mutagenesis method, we generated a leptin-deficient *Lep^{mkyo}/Lep^{mkyo}* rat that had a nonsense mutation (Q92X) in leptin gene. *Lep^{mkyo}/Lep^{mkyo}* rats showed obese phenotypes including severe fatty liver, which were comparable to *Lep^{ob}/Lep^{ob}* mice. To identify genes that respond to leptin in the liver, we performed microarray analysis with *Lep^{mkyo}/Lep^{mkyo}* rats and *Lep^{ob}/Lep^{ob}* mice. We sorted out genes whose expression levels in the liver of *Lep^{mkyo}/Lep^{mkyo}* rats were changed from wild-type (WT) rats and were reversed toward WT rats by leptin administration. In this analysis, livers were sampled for 6 h, a relatively short time after leptin administration to avoid the secondary effect of metabolic changes such as improvement of fatty liver. We did the same procedure in *Lep^{ob}/Lep^{ob}* mice and selected genes whose expression patterns were common in rat and mouse. We verified their gene expressions by real-time quantitative PCR. Finally, we identified eight genes that primarily respond to leptin in the liver commonly in rat and mouse. These genes might be important for the effect of leptin in the liver.

ENU mutagenesis; *Lep^{mkyo}/Lep^{mkyo}* rat; *Lep^{ob}/Lep^{ob}* mouse; leptin responsive gene; microarray analysis

LEPTIN IS AN ADIPOCYTE-DERIVED hormone that regulates energy homeostasis mainly through the hypothalamus (1). In addition to food intake and energy expenditure, leptin regulates glucose and lipid metabolism (5, 13, 20). Leptin-deficient *Lep^{ob}/Lep^{ob}* mice are well known to have made a great contribution in the discovery of leptin, and they have been used as an animal model of obesity and obesity-associated diabetes mellitus. Although much has been learned from *Lep^{ob}/Lep^{ob}* mice, it is important to use other models of different species to generalize results from one species.

For the last 30 yr, many investigators have chosen to use mouse models, because the technologies of embryonic stem

cells allowed the generation of knockout and knock-in mice (7). However, rats have a long history in medical research, being fundamental from drug development to advances of neuroscience and physiology. Rats are considered to be a better model than mice in their behavioral and physiological characteristics, which are more relevant to humans.

Lep^{fa}/Lep^{fa} Zucker rats and *Lep^r/Lep^r* Koletzky rats already exist as rat models whose lack of leptin signals is due to mutations in the leptin receptor (22, 23). The phenotypes in these rats are also identical in many aspects to those in *Lep^{ob}/Lep^{ob}* mice (4). However, leptin receptor mutant rats are unfit models for the study of the effect of leptin treatment. Although generation of leptin knockout rats by pronuclear microinjections of zinc finger nucleases has been reported recently (26), the investigators did not assess the effect of leptin administration. So this is the first report of leptin administration in the leptin-deficient rat.

In this study, we used the *N*-ethyl-*N*-nitrosourea (ENU) mutagenesis method to generate a leptin-deficient *Lep^{mkyo}/Lep^{mkyo}* rat that had a nonsense mutation (Q92X) in the leptin gene (17). The mutation site of *Lep^{mkyo}/Lep^{mkyo}* rat was upstream of that of R105X in *Lep^{ob}/Lep^{ob}* mice (28). We confirmed that *Lep^{mkyo}/Lep^{mkyo}* rats secreted no measurable leptin in the serum and that their obese phenotypes including severely fatty liver were comparable to *Lep^{ob}/Lep^{ob}* mice. To identify genes that respond to leptin in the liver, we compared gene expressions in the liver between *Lep^{mkyo}/Lep^{mkyo}* rats and their wild-type (WT) littermates and also between leptin-treated and saline-treated *Lep^{mkyo}/Lep^{mkyo}* rats by microarray analysis. We sorted out genes whose expression levels in the liver of *Lep^{mkyo}/Lep^{mkyo}* rats were changed from WT rats and were reversed toward WT rats by leptin treatment. Moreover, to identify genes that commonly respond to leptin in the liver of rats and mice, we did the same series of experiments with *Lep^{ob}/Lep^{ob}* mice. We finally identified eight genes that commonly respond to leptin in the liver of rats and mice. Using more than one species can improve the accuracy of analysis results. Thus, genes identified in this study might be important for the effect of leptin in the liver.

MATERIALS AND METHODS

Animals. Rats with a leptin gene mutation were obtained by ENU mutagenesis of F344/NSlc rats, followed by MuT-POWER (Mu Transposition POoling method With sequencER) screening on the genomic DNA of 4,608 G1 male offspring in KURMA (Kyoto University Rat Mutant Archive). ENU mutagenesis procedures, screening protocols

Address for reprint requests and other correspondence: K. Ebihara, Dept. of Experimental Therapeutics, Translational Research Center, Kyoto Univ. Hospital, 54 Shogoin Kawahara-cho, Sakyo-ku, Kyoto 606-8507, Japan (e-mail: kebihara@kuhp.kyoto-u.ac.jp).

GAGTCCACCTTGCG-3', rat 18s (F) 5'-GCAATTATCCCCATGAACGA-3', rat 18s (R) 5'-CAAAGGGCAGGGACTTAATCAAC-3', probe: 5'-AATTCCCAGTAAGTGCGGGTCATAAGCTTG-3', mouse 18s (F) 5'-CGCGCAAATTACCCACTCCCGA-3', mouse 18s (R) 5'-CGGCTACCACATCCAAGGA-3', probe: 5'-CCAATTACAGGGCCTCGAAA-3'.

Statistical analysis. Data are expressed as means \pm SE. Comparison between or among groups was assessed by Student's *t*-test or ANOVA with Fisher's protected least significant difference test. $P < 0.05$ was considered statistically significant. The χ^2 -test was used for analysis of genotype and sex ratio using Microsoft Excel. $P < 0.05$ was considered statistically significant.

RESULTS

Generation of a novel genetically obese rat with a homozygous nonsense mutation in the leptin gene. By using ENU mutagenesis followed by MuT-POWER screening of the KURMA samples (17), we generated a genetically obese *Lep^{mk_{yo}}/Lep^{mk_{yo}}* rat with a homozygous nonsense mutation in the leptin gene. *Lep^{mk_{yo}}* mutation was a C-to-T transition at nucleotide 274 in the third exon of leptin gene, resulted to a substitution of glutamine at codon 92 by the stop codon (Q92X), which is upstream of the mutation (R105X) in *Lep^{ob}/Lep^{ob}* mice (28) (Fig. 1). Male and female *Lep^{mk_{yo}}/+* rats were intercrossed to obtain WT, *Lep^{mk_{yo}}/+*, and *Lep^{mk_{yo}}/Lep^{mk_{yo}}* animals. There were 27 homozygous WT, 40 *Lep^{mk_{yo}}/+*, and 16 *Lep^{mk_{yo}}/Lep^{mk_{yo}}* rats. This ratio did not differ significantly from the expected 1:2:1 Mendelian ratio of genotypes (delivery $n = 8$, mean n of pups per delivery = 10.25; $\chi^2 = 3.17$, $P = 0.999$). The sex ratios also did not differ significantly from the expected ratio (male $n = 42$, female $n = 40$, $\chi^2 = 2.42$, $P = 0.93$).

Plasma leptin concentration and obese phenotypes in *Lep^{mk_{yo}}/Lep^{mk_{yo}}* rats. ELISA did not detect plasma leptin in *Lep^{mk_{yo}}/Lep^{mk_{yo}}* rats (Fig. 2A). Serum leptin concentration in *Lep^{mk_{yo}}/+* rats (7.81 ± 0.74 ng/ml) was slightly higher than half that of WT rats (12.17 ± 0.72 ng/ml). The body weight in *Lep^{mk_{yo}}/Lep^{mk_{yo}}* rats was significantly heavier than WT rats as early as

5 wk of age (Fig. 2B). The difference in body weight between WT and *Lep^{mk_{yo}}/Lep^{mk_{yo}}* rats steadily widened throughout the study period. The body weight in *Lep^{mk_{yo}}/+* rats was always slightly heavier than that in WT rats although the difference was not statistically significant. As for the body length, there was no difference between WT and *Lep^{mk_{yo}}/Lep^{mk_{yo}}* rats (22.63 ± 0.13 cm in WT rats and 22.69 ± 0.24 cm in *Lep^{mk_{yo}}/Lep^{mk_{yo}}* rats, $n = 7$, $P = 0.86$), unlike *Lep^{ob}/Lep^{ob}* mice in which the body length is 5–10% shorter than that in lean littermates (3). The gross appearances of WT, *Lep^{mk_{yo}}/+*, and *Lep^{mk_{yo}}/Lep^{mk_{yo}}* rats at the age of 19 wk are shown in Fig. 2C. The body composition was examined with computer tomography (Fig. 2D). In *Lep^{mk_{yo}}/Lep^{mk_{yo}}* rats, the subcutaneous fat mass was nearly four times and the intra-abdominal fat mass was nearly twice of those in WT rats. Both subcutaneous fat mass and intra-abdominal fat mass in *Lep^{mk_{yo}}/+* rats were slightly greater than those in WT rats. Daily food intake in *Lep^{mk_{yo}}/Lep^{mk_{yo}}* rats was increased by ~50% compared with WT rats (Fig. 2E). The mean body temperature in *Lep^{mk_{yo}}/Lep^{mk_{yo}}* rats was significantly lower than that in WT rats (Fig. 2F). There was no significant difference between WT and *Lep^{mk_{yo}}/+* rats in both food intake and body temperature.

Glucose and lipid metabolism in *Lep^{mk_{yo}}/Lep^{mk_{yo}}* rats. We performed intraperitoneal glucose tolerance test (Fig. 3, A and B). Before glucose load, both plasma glucose and insulin concentrations in *Lep^{mk_{yo}}/Lep^{mk_{yo}}* rats were already increased when compared with those in WT rats. Plasma glucose concentration in response to the glucose load in *Lep^{mk_{yo}}/Lep^{mk_{yo}}* rats was also significantly higher than WT rats. Moreover, the increment of plasma insulin concentration was sustained after glucose load in *Lep^{mk_{yo}}/Lep^{mk_{yo}}* rats. These results indicate that the main cause of the impairment of glucose tolerance in *Lep^{mk_{yo}}/Lep^{mk_{yo}}* rats was insulin resistance. No significant difference between WT and *Lep^{mk_{yo}}/+* rats in both plasma glucose and insulin concentrations was observed during glucose tolerance test.

Compared with WT rats, the fasting plasma triglyceride concentration in *Lep^{mk_{yo}}/Lep^{mk_{yo}}* rats was markedly elevated (Fig. 3C). The NEFA concentration was also increased in *Lep^{mk_{yo}}/Lep^{mk_{yo}}* rats although there was no significant difference (Fig. 3D). Plasma total cholesterol concentration was significantly increased in *Lep^{mk_{yo}}/Lep^{mk_{yo}}* rats (Fig. 3E). There was no significant difference between WT and *Lep^{mk_{yo}}/+* rats in any of these plasma lipid concentrations.

Liver phenotype in *Lep^{mk_{yo}}/Lep^{mk_{yo}}* rats. In *Lep^{mk_{yo}}/Lep^{mk_{yo}}* rats, the liver was markedly enlarged and lighter in color than that in WT rats. Histological examination of the liver showed large number of lipid droplets of various sizes in *Lep^{mk_{yo}}/Lep^{mk_{yo}}* rats (Fig. 3F). There was no accumulation of lipid droplets in *Lep^{mk_{yo}}/+* rats. Consistent with these observations, both liver weight and liver triglyceride content in *Lep^{mk_{yo}}/Lep^{mk_{yo}}* rats were markedly increased compared with those in WT rats (Fig. 3, G and H). There was no significant difference between WT and *Lep^{mk_{yo}}/+* rats in both liver weight and liver triglyceride content.

Identification of leptin-responsive genes in the liver by microarray analyses. To identify leptin-responsive genes in the liver, we compared gene expressions in the liver between *Lep^{mk_{yo}}/Lep^{mk_{yo}}* rats and their WT littermates, as well as leptin-treated and saline-treated *Lep^{mk_{yo}}/Lep^{mk_{yo}}* rats, by the microarray method. In the leptin administration experiment, to avoid the effect of chronic

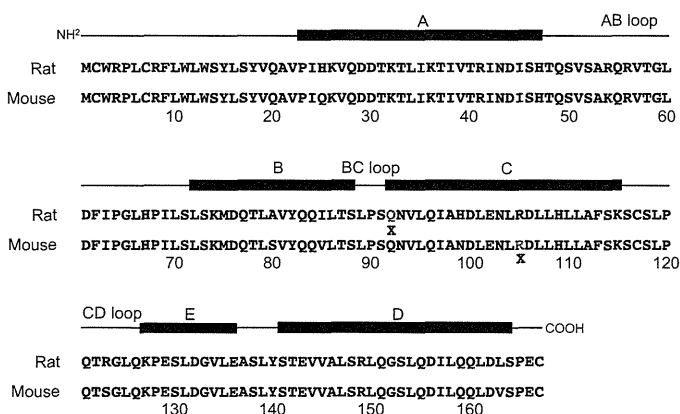


Fig. 1. Mutation (Q92X) in *Lep^{mk_{yo}}/Lep^{mk_{yo}}* rats is upstream of the mutation (R105X) in *Lep^{ob}/Lep^{ob}* mice. Secondary structure elements (top) of leptin precursor and its amino acid sequence in rat (middle) and mouse (bottom). There is 96% identity of amino acid sequence between mouse and rat. It consists of 4 antiparallel α -helices (A, B, C, and D), connected by 2 long crossover loops (AB and CD) and 1 short loop (BC). Leptin has a small distorted helical segment E in the CD loop. The red Q in the rat sequence indicates the amino acid position of the Q92X mutation. The red R in the mouse sequence indicates the amino acid position of the R105X mutation.

(17), and intracytoplasmic sperm injection procedure were previously described (12). The forward primer and the reverse primer used for identifying mutation of the leptin gene were 5'-GCACCTGTTGTTCTCTTCC-3' and 5'-TGGAAATCGTGGGATAAAGTT-3', respectively. More than six backcross generations were performed against the F344/NSlc inbred background. Male C57Bl/6J *Lep^{ob}/Lep^{ob}* mice were purchased from CLEA Japan (Tokyo, Japan). Rats and mice were maintained on a 10 h light/14 h dark cycle (lights on 7:00 AM, lights off 9:00 PM) and fed ad libitum standard pellet diet (MF; Oriental Yeast, Tokyo, Japan). All animal care and experiments conformed to the Guidelines for Animal Experiments at Kyoto University and were approved by the Animal Research Committee of Kyoto University. The F344-*Lep^{mkyo}* rat has been deposited into the National Bio Resource Project-Rat in Japan (NBPR-Rat no. 0628) and is available from the Project (<http://www.anim.med.kyoto-u.ac.jp/nbr>).

Genotyping for *Lep^{mkyo}* mutation. Genotyping for *Lep^{mkyo}* mutation was performed by real-time PCR system using TaqMan Sample-to-SNP kit (Applied Biosystems, Carlsbad, CA) with a specific primer pair (forward primer sequences are 5'-GTTCTCCAGGTCATGAGC-TATCTG-3' and reverse primer sequences are 5'-CTGGCAGTC-TATCAACAGATCCT-3') and TaqMan MGB probes (WT probe sequences are 5'-TTGCCTTCCCAAACG-3' and mutant probe sequences are 5'-TTGCCTTCCCAAACG-3'). Genomic DNA was extracted from whole blood. The cycling conditions were 20 s at 95°C followed by 40 cycles of 3 s at 95°C and 20 s at 60°C.

Whole body composition analysis. Twenty-week-old male rats under anesthesia were scanned from nose to anus by computer tomography with La Theta LCT-100 (Aloka, Tokyo, Japan). The X-ray source tube voltage was set at 50 kV with a constant 1 mA current. Aloka software estimated the volume of adipose tissue, bone, air, and the remainder using differences in X-ray density. Distinguishing intra-abdominal adipose tissue and subcutaneous adipose tissue was based on detection of the abdominal muscle layers. Fat weight was calculated using the commonly used density factor of 0.92 g/cm³. This method provides accurate estimation of total subcutaneous and intra-abdominal fat pads as validated by dissection (11).

Measurement of body length and rectal temperature. Body length was measured between nose and anus in 19-wk-old male rats under anesthesia. Rectal temperature was measured with a digital thermometer (BDT-100; Bio Research Center, Tokyo, Japan) at 10:00 AM in 19 wk old male rats.

Biochemical assays. Blood was obtained from the tail vein after overnight fasting at the age of 19 wk. Plasma leptin concentrations were measured by an enzyme-linked immunosorbent assay (ELISA) kit for rat leptin (Millipore, St. Charles, MO). Plasma glucose concentrations were measured by a glucose assay kit (Wako Pure Chemical Industries, Osaka, Japan). Plasma insulin concentrations were measured by an insulin-ELISA kit (Morinaga Institute of Biological Science, Yokohama, Japan). Plasma triglyceride, nonesterified fatty acid (NEFA), and total cholesterol concentrations were measured by enzymatic kits (Triglyceride E-test Wako, NEFA C-test Wako, and Cholesterol E-test Wako, respectively; Wako Pure Chemical Industries). To measure liver triglyceride contents, we sampled livers from 19 wk old rats and immediately froze them in liquid nitrogen. Lipids were extracted with isopropyl alcohol-heptane (1:1 vol/vol). After evaporating the solvent, we resuspended lipids in 99.5% (vol/vol) ethanol, and triglyceride content was measured by an enzymatic kit (Triglyceride E-test Wako, Wako Pure Chemical Industries).

Glucose tolerance test. Intraperitoneal glucose tolerance test was performed after overnight fasting of 19 wk old male rats. Rats received 2.0 mg/g glucose by intraperitoneal injection. Blood was sampled from the tail vein before and 15, 30, 60, 90, 120 min after the glucose load.

Liver histology. Livers were sampled from 19 wk old rats, fixed in 10% neutrally buffered formalin, and subsequently embedded in paraffin. Histological sections of 5 μm thickness were stained with hematoxylin and eosin and examined by light microscopy.

Liver sampling for microarray analysis. Recombinant murine leptin (generously supplied by Amgen, Thousand Oaks, CA) (1 μg/mg) or saline was intraperitoneally administered in 20 wk old *Lep^{ob}/Lep^{ob}* mice, *Lep^{mkyo}/Lep^{mkyo}* rats and their respective control littermates after 6 h fasting. Livers were sampled 6 h after leptin or saline administration and were frozen in liquid nitrogen and stored at -80°C until use for RNA isolation.

RNA extraction and microarray gene expression arrays. Details for the sample preparation and microarray processing are available from <http://www.affymetrix.com>. RNA was prepared from liver of three male mice or rats per group using Trizol (Invitrogen, Carlsbad, CA) reagent following the supplier's protocol. The quality and the concentrations of the extracted RNA were checked using the Nano-Drop 2000 (Thermo Fisher Scientific, Yokohama, Japan). Each three RNA samples were pooled for analysis. We used 250 ng of total RNA for one cycle of cDNA synthesis. Hybridization, washing, and scanning of Affymetrix GeneChip Mouse Genome 430 2.0 Arrays (Affymetrix, Santa Clara, CA) and Affymetrix GeneChip Rat Genome 230 2.0 Arrays were done according to standard Affymetrix protocols. The hybridized chips were scanned with an argon-ion laser confocal microscope (Hewlett-Packard, Palo Alto, CA). Fluorometric data were processed by Affymetrix GeneChip Command Console software and analyzed with Affymetrix Expression Console software 7. Normalization was performed with Affymetrix Microarray Suite 5.0 (MAS5.0) algorithm to obtain the signal intensity and the detection call, which shows the expression of a gene with a defined confidence level for each probe set. The mRNA expression levels for all genes on the array were scaled to a mean of 500 for each array. The detection call can be "present" when the perfect match probes are significantly more hybridized than the mismatch probes, false discovery rate (FDR) < 0.04, "marginal" for FDR > 0.04, and <0.06 or "absent," FDR > 0.06.

Real-time quantitative RT-PCR. Real-time quantitative RT-PCR was performed to validate expression levels of candidate leptin-responsive genes. Single-stranded cDNA was synthesized from 1 μg of total RNA using SuperScript III First-Strand Synthesis System for RT-PCR, according to the manufacturer's instructions (Invitrogen). Quantitative RT-PCR was performed with SYBR Green (Applied Biosystems) by Applied Biosystems StepOnePlus RT-PCR System using gene-specific primer. The housekeeping rat or mouse mitochondrial subunit 18S rRNA genes were used for control and quantitative RT-PCR was performed with TaqMan (Applied Biosystems). The sequences of primers (Sigma-Genosys, Tokyo, Japan) used in the present study are as follows: rat *Ccl2* (F) 5'-TAGCATCCACGTGCTGTCTC-3', rat *Ccl2* (R) 5'-CAGCCGATCATTGGGATCA-3', mouse *Ccl2* (F) 5'-AGATG-CAGTTAACGCCCCAC-3', mouse *Ccl2* (R) 5'-GACCCATTCCTTCT-TGGGGT-3', rat *Cdca3* (F) 5'-AACAAAGCATGTGTCTCGGGT-3', rat *Cdca3* (R) 5'-TCTTGGCCTGTTTGGAGACT-3', mouse *Cdca3* (F) 5'-CCTCGTTACCTAGTGCTGG-3', mouse *Cdca3* (R) 5'-TTTCGTCT-GCTGCGCTTAGA-3', rat *Fkbp5* (F) 5'-ACTGACTCGCCTGACA-CAAG-3', rat *Fkbp5* (R) 5'-GAGCAGGTATCTGCTGTCTGTC-3', mouse *Fkbp5* (F) 5'-CTTGGACCACGATGTTT-3', mouse *Fkbp5* (R) 5'-GGATTGACTGCCAACACCTT-3', rat *Inhbb* (F) 5'-TCACGGTGA-CAGGTGGAATG-3', rat *Inhbb* (R) 5'-CCGTTTTTCGGATGCGATGTC-3', mouse *Inhbb* (F) 5'-TGACCCACACTAGGCGAAAC-3', mouse *Inhbb* (R) 5'-CAGGCCACTCGAAGGATTGT-3', rat *Lin7a* (F) 5'-AAGCCA-CAAGAATCCGGAGA-3', rat *Lin7a* (R) 5'-CTGACGACCAGCTTCA-CACT-3', mouse *Lin7a* (F) 5'-AGTACCAGTGCACAAGCTCC-3', mouse *Lin7a* (R) 5'-CATGTCTTTTACGCCACCCT-3', rat *C-Myc* (F) 5'-ATTCCAGCGAGAGACAGAGGGAGTG-3', rat *C-Myc* (R) 5'-ACGTTGAGGGGCATCGTCTGTG-3', mouse *C-Myc* (F) 5'-CGCGC-CCAGTGAGGATATC-3', mouse *C-Myc* (R) 5'-CCACATACAGTC-CTGGATGAT-3', rat *Npr2* (F) 5'-TTGGGGAGAGTCTACGACAG-3', rat *Npr2* (R) 5'-CTCGGTACGTGATCACCAGG-3', mouse *Npr2* (F) 5'-CCAGAAGTCTTAGCGGGAA-3', mouse *Npr2* (R) 5'-CTGAC-CATTCCGCACCTTCT-3', rat *Ppl* (F) 5'-AGTGCTGCCACTCAAG-TACC-3', rat *Ppl* (R) 5'-CAGCTCTCCCCGTGTTCTT-3', mouse *Ppl* (F) 5'-GCATGCTGAGTGGAAAGGAGT-3', mouse *Ppl* (R) 5'-AAGTCT-

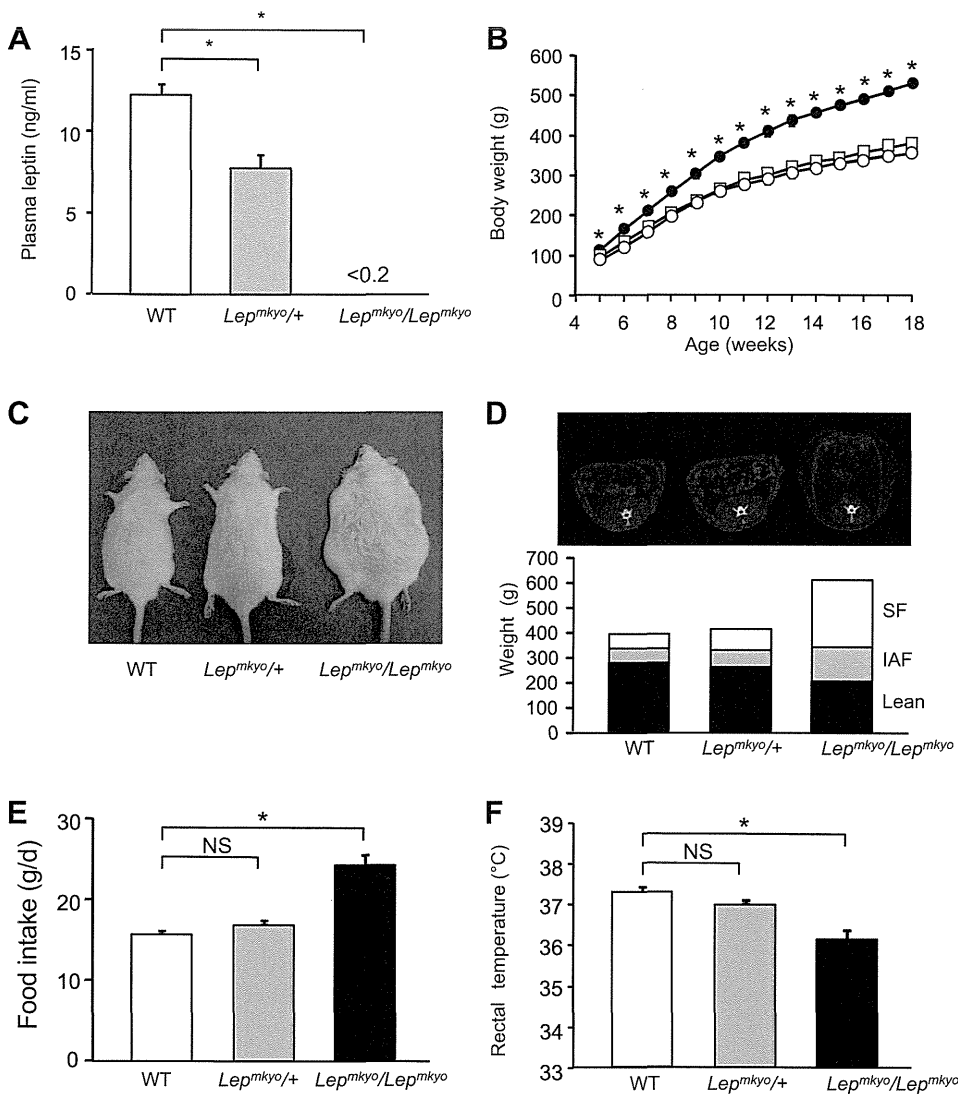


Fig. 2. Obese phenotypes of *Lep^{mkycy}/Lep^{mkycy}* rats. **A:** plasma leptin concentrations in wild-type (WT, open bar), *Lep^{mkycy}/+* (gray bar), and *Lep^{mkycy}/Lep^{mkycy}* (closed bar) rats. Data are means \pm SE ($n = 4$ each group). * $P < 0.01$ (Student's *t*-test). **B:** growth curves in WT (\circ), *Lep^{mkycy}/+* (\square), and *Lep^{mkycy}/Lep^{mkycy}* (\bullet) rats. Data are means \pm SE ($n = 4$ each group). * $P < 0.05$ (ANOVA). **C:** gross appearance of WT, *Lep^{mkycy}/+*, and *Lep^{mkycy}/Lep^{mkycy}* rats. **D:** computer tomography (CT) image at a slice 15 cm distal from nose (top) and body composition in WT, *Lep^{mkycy}/+*, and *Lep^{mkycy}/Lep^{mkycy}* rats (bottom). SF, subcutaneous fat mass; IAF, intra-abdominal fat mass; Lean, lean body mass. **E:** daily food intake in WT (open bar), *Lep^{mkycy}/+* (gray bar), and *Lep^{mkycy}/Lep^{mkycy}* (closed bar) rats. Daily food intake was measured at the age of 19 wk. Data are means \pm SE ($n = 4$ each group). * $P < 0.05$ (Student's *t*-test). NS, not significant. **F:** rectal temperature in WT (open bar), *Lep^{mkycy}/+* (gray bar), and *Lep^{mkycy}/Lep^{mkycy}* (closed bar) rats. Data are means \pm SE ($n = 4$ each group). * $P < 0.05$ (Student's *t*-test).

metabolic changes related to food intake and body weight suppressions by leptin, we administered leptin and started rats fasting at the same time, 6 h before the liver sampling. Moreover, to identify genes that commonly respond to leptin in the liver in rats and mice, we did the same series of experiments with *Lep^{ob}/Lep^{ob}* mice. We confirmed that there was no significant difference in body weight and plasma glucose, insulin and triglyceride concentrations between leptin-treated and saline-treated *Lep^{mkycy}/Lep^{mkycy}* rats and also between leptin-treated and saline-treated *Lep^{ob}/Lep^{ob}* mice (data not shown).

Of 31,042 genes in the rat array chip, we excluded from analysis 18,425 genes with no nomenclature, which could not be found in the mouse array chip, and whose detection calls were not present in any of WT, *Lep^{mkycy}/Lep^{mkycy}*, and leptin-treated *Lep^{mkycy}/Lep^{mkycy}* rats. Of the remaining 12,617 genes, 177 genes whose expressions were decreased >1.6 -fold in *Lep^{mkycy}/Lep^{mkycy}* rats relative to WT rats and increased >1.6 -fold in leptin-treated *Lep^{mkycy}/Lep^{mkycy}* rats relative to saline-treated *Lep^{mkycy}/Lep^{mkycy}* rats were defined as leptin-upregulated genes in rat. However, 138 genes whose expression levels were <100 in either WT or *Lep^{mkycy}/Lep^{mkycy}* rats were excluded. We defined 237 genes whose expressions were increased >1.6 -

fold in *Lep^{mkycy}/Lep^{mkycy}* rats relative to WT rats and decreased >1.6 -fold in leptin-treated *Lep^{mkycy}/Lep^{mkycy}* rats relative to saline-treated *Lep^{mkycy}/Lep^{mkycy}* rats as leptin-downregulated genes in rat. In this case, 158 genes whose expression levels were <100 in saline-treated *Lep^{mkycy}/Lep^{mkycy}* rats were excluded from leptin-downregulated genes. Furthermore, among 39 leptin-upregulated genes in rat, six genes whose expression was decreased >1.6 -fold in *Lep^{ob}/Lep^{ob}* mice relative to WT mice and increased >1.0 -fold in leptin-treated *Lep^{ob}/Lep^{ob}* mice relative to saline-treated *Lep^{ob}/Lep^{ob}* mice were defined as leptin-upregulated genes common in rat and mouse. Among 79 leptin-downregulated genes in rat, 14 genes whose expression were increased >1.6 -fold in *Lep^{ob}/Lep^{ob}* mice relative to WT mice and decreased >1.0 -fold in leptin-treated *Lep^{ob}/Lep^{ob}* mice relative to saline-treated *Lep^{ob}/Lep^{ob}* mice were defined as leptin-downregulated genes common in rat and mouse.

Expression patterns of these 20 leptin-regulated genes common in rat and mouse were examined by quantitative RT-PCR using the same RNA samples used for microarray analysis. Among six leptin-upregulated genes, *Lin7a* and *Npr2* showed a similar expression pattern in microarray and quantitative RT-PCR analysis (Table 1, Fig. 4A). Among 14 leptin-downregulated genes in rats,

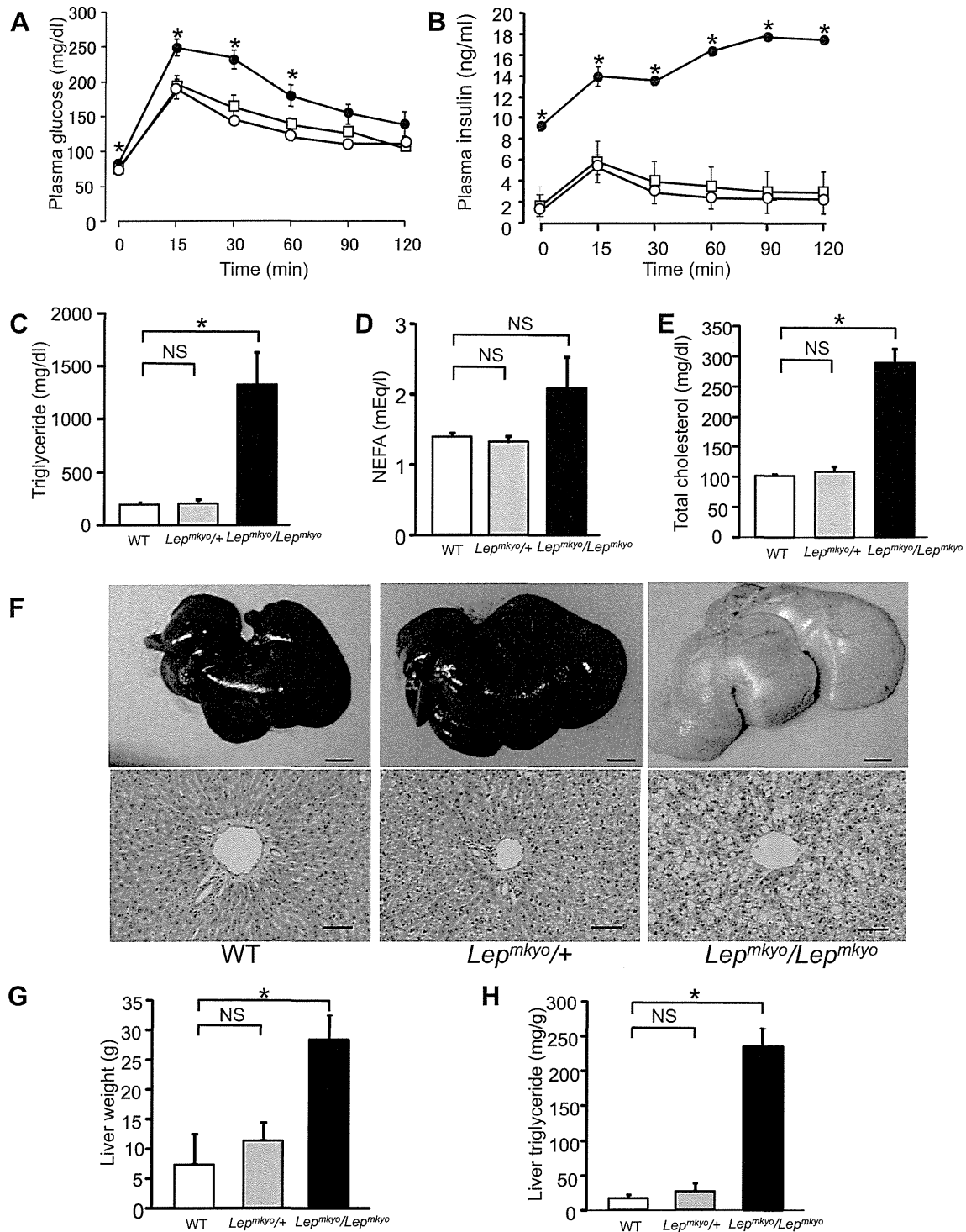


Fig. 3. Glucose, lipid metabolism, and fatty liver in *Lep^{mkyo}/Lep^{mkyo}* rats. Plasma glucose (A) and insulin concentrations (B) at intraperitoneal glucose tolerance test in WT (○), *Lep^{mkyo}/+* (□), and *Lep^{mkyo}/Lep^{mkyo}* (●) rats. Data are means \pm SE ($n = 4$ each group). * $P < 0.05$ (ANOVA). Plasma triglyceride (C), nonesterified fatty acid (NEFA, D), and total cholesterol (E) concentrations in WT (open bar), *Lep^{mkyo}/+* (gray bar), and *Lep^{mkyo}/Lep^{mkyo}* (closed bar) rats. Data are means \pm SE ($n = 4$ each group). * $P < 0.05$ (Student's *t*-test). F: representative macroscopic (top: scale bar, 1 cm) and histological (bottom: scale bar, 100 μ m) sections of the liver in WT, *Lep^{mkyo}/+*, and *Lep^{mkyo}/Lep^{mkyo}* rats. For histological examination, hematoxylin and eosin staining was used. Liver weight (G) and liver triglyceride contents (H) in WT (open bar), *Lep^{mkyo}/+* (gray bar), and *Lep^{mkyo}/Lep^{mkyo}* (closed bar) rats. Data are means \pm SE ($n = 4$ each group). * $P < 0.01$ (Student's *t*-test).

Table 1. *Microarray analysis data of leptin-responsive genes in the liver*

Gene Name	Gene Symbol	UniGene (Rn.)		Fold Increase			
		Rat (Rn.)	Mouse (Mm.)	Rat		Mouse	
				Wild/ <i>Lep^{mk_{yo}}/Lep^{mk_{yo}}</i>	Leptin/vehicle	Wild/ <i>ob/ob</i>	Leptin/vehicle
<i>Leptin-upregulated gene in liver</i>							
Lin-7 homolog A (<i>C. elegans</i>)	Lin7a	31766	268025	2.014	2.158	1.729	1.404
Natriuretic peptide receptor 2	Npr2	32984	103477	2.567	2.25	4.627	1.064
<i>Leptin-downregulated gene in liver</i>							
Chemokine (C-C motif) ligand 2	Ccl2	4772	290320	0.202	0.54	0.17	0.871
Cell division cycle associated 3	Cdca3	129078	285723	0.23	0.207	0.432	0.382
FK506 binding protein 5	Fkbp5	144288	276405	0.219	0.536	0.401	0.774
G protein-coupled receptor 64	Gpr64	57243	213016	0.105	0.574	0.129	0.853
Inhibin beta-B	Inhbb	35074	3092	0.016	0.603	0.33	0.871
Myelocytomatosis oncogene	Myc	12072	2444	0.299	0.473	0.398	0.595
Periplakin	Ppl	25259	266875	0.23	0.547	0.536	0.768

Ccl2, *Cdca3*, *Fkbp5*, *Inhbb*, *C-Myc*, and *Ppl* showed similar expression patterns between microarray and quantitative RT-PCR analysis (Table 1, Fig. 4B). These eight genes are expected to play some role in the effect of leptin on the liver.

All microarray data have been deposited at the National Center for Biotechnology Information in the Gene Expression Omnibus database (GEO, <http://www.ncbi.nlm.nih.gov/geo/>). The series accession number is GSE42532. The GEO platform accession number is GPL1261 in mouse, GPL1355 in rat. The sample accession numbers are GSM 1044286, 1044287, 1044288, 1044289, 1044290, and 1044291.

DISCUSSION

Using gene-driven ENU mutagenesis, we generated leptin-deficient *Lep^{mk_{yo}}/Lep^{mk_{yo}}* rat. The mutation of leptin gene in *Lep^{mk_{yo}}/Lep^{mk_{yo}}* rats is located at nucleotide 274 in the third exon of leptin gene, generating a stop codon at amino acid 92 (Q92X), which is upstream of the mutation (R105X) in *Lep^{ob}/Lep^{ob}* mice (28). Leptin contains two cysteine residues, Cys96 and Cys146, which form a disulfide bond. This disulfide bond was shown to be required for the leptin action (27). Since both sites of nonsense mutation in *Lep^{mk_{yo}}/Lep^{mk_{yo}}* rats and *Lep^{ob}/Lep^{ob}* mice were projected to disrupt this disulfide bond, *Lep^{mk_{yo}}/Lep^{mk_{yo}}* rats were considered to have no functional leptin, as well as *Lep^{ob}/Lep^{ob}* mice.

The mean mutation frequency with ENU mutagenesis of our protocol was one mutation per 3.7 million base pairs (17). Although the chance for the occurrence of an unexpected mutation with a phenotypic effect is relatively small, this possibility also should be taken account for the experimental design and interpretation of the results. To eliminate mutations that might have been generated by ENU in chromosomal regions other than the *Lep* locus, we performed backcross more than six generations against F344/NSlc inbred background, and we always compared phenotypes between littermates to minimize the effect of possible unexpected mutation.

Lep^{mk_{yo}}/Lep^{mk_{yo}} rats showed morbid obesity with hyperphagia and low body temperature, hyperglycemia with hyperinsulinemia, dyslipidemia, and severely fatty liver. Low body temperature suggests decreased sympathetic nervous activity and basal metabolism in *Lep^{mk_{yo}}/Lep^{mk_{yo}}* rats. The glucose tolerance test demonstrated marked glucose intolerance with sus-

tained hyperinsulinemia in *Lep^{mk_{yo}}/Lep^{mk_{yo}}* rats, suggesting insulin resistance. All these phenotypes are consistent with the lack of functional leptin and are identical to those in *Lep^{ob}/Lep^{ob}* mice (4). There are some existing rat models, such as *Lep^{fa}/Lep^{fa}* Zucker rats and *Lep^r/Lep^r* Koletzky rats, whose lack of leptin signals is due to mutations in the leptin receptor (22, 23). Although the phenotypes of these rats are also identical to *Lep^{mk_{yo}}/Lep^{mk_{yo}}* rats, they are not useful in studying the effect of leptin treatment. In this study, we used *Lep^{mk_{yo}}/Lep^{mk_{yo}}* rat as a leptin-treatable rat model and showed its usefulness.

Generation of leptin knockout rats by pronuclear microinjections of zinc finger nucleases had been reported recently (26). In addition to the metabolic phenotype, those leptin knockout rats with Sprague-Dawley background showed significant increase in bone mineral density and bone volume of the femur compared with WT littermates like *ob/ob* mice (26). However, we could not detect any significant difference in bone mineral density and gross observation of trabecular in the femur by computer tomography between *Lep^{mk_{yo}}/Lep^{mk_{yo}}* rats and their WT littermates (data not shown). Our result is consistent with the previous report on leptin receptor mutated *fa/fa* rats with Zucker background (24). These results indicate the strain difference in the regulation of bone mineral density. Furthermore, there is a previous report that bone mass in patients with congenital leptin deficiency have normal or low bone mineral density (18), which indicates the species difference. It was also reported that T-cell count was decreased in those leptin knockout rats. In all previous reports of leptin or leptin receptor deficiency in humans (9), mice (16), and rats (25), T-cell count was also decreased. As for the phenotype of T-cell, there is no difference between strains or species, although we did not count the T cells in *Lep^{mk_{yo}}/Lep^{mk_{yo}}* rats.

Besides the antiobesity effect, leptin has a wide range of metabolic effects including an insulin-sensitizing action. However, the molecular mechanism underlying metabolic effects of leptin is not well understood. We and others have demonstrated that leptin effectively improves insulin sensitivity accompanied by a dramatic reduction of fat content in the liver and skeletal muscle in patients with lipodystrophy in which severely fatty liver and excess fat accumulation in the skeletal muscle frequently develop (5, 6, 8, 15). In this study, to investigate the molecular mechanism by which leptin reduces fat content in the liver, we

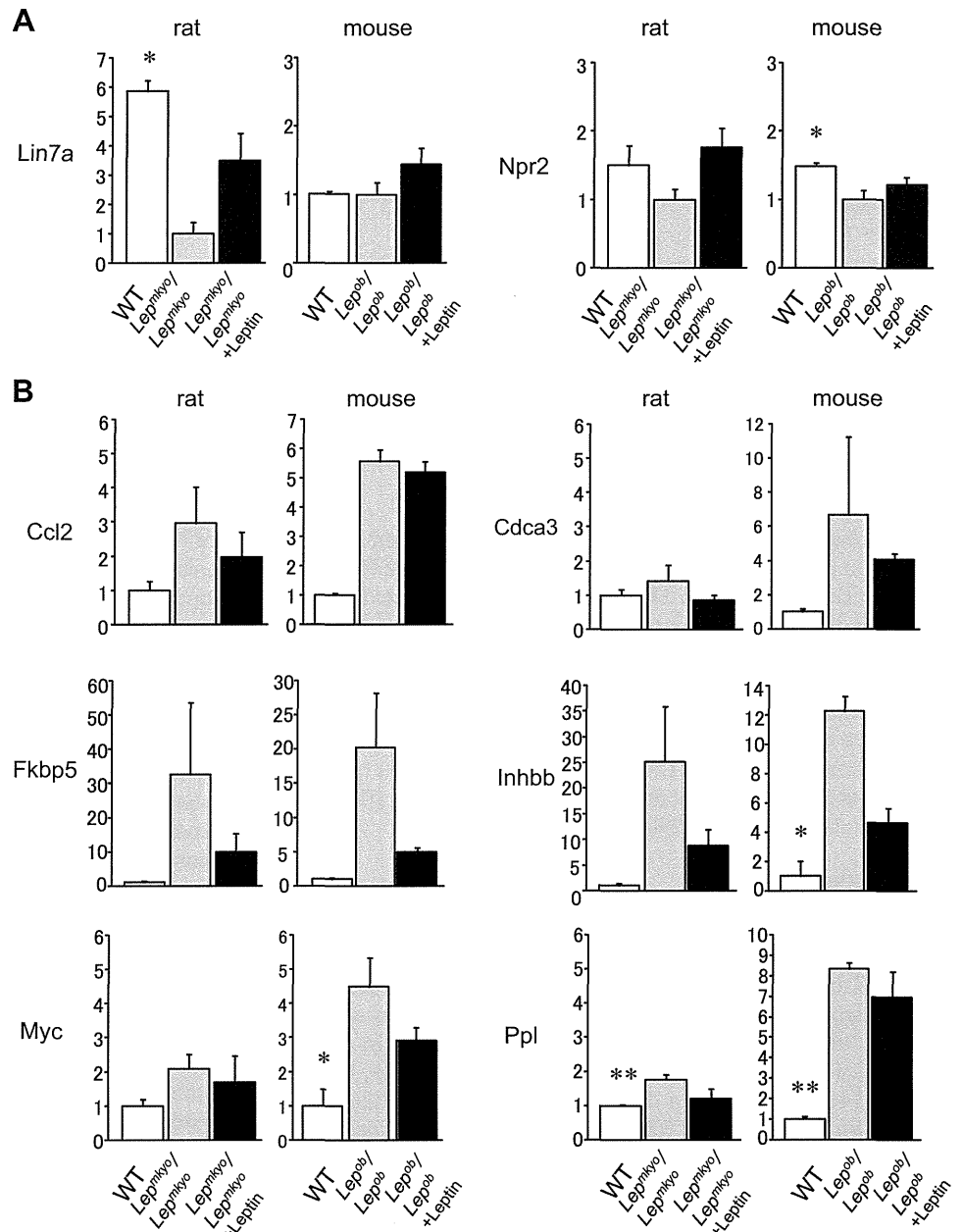


Fig. 4. Reproducibility with quantitative RT-PCR in mRNA expression. The leptin-up-regulated genes common in rats and mice (A) and leptin-downregulated genes common in rats and mice (B) were checked for reproducibility with quantitative RT-PCR. The fold change was displayed as relative to normalized to leptin-deficient animals in A and as relative to WT animals in B. * $P < 0.05$, ** $P < 0.01$ (Student's *t*-test). *Lin7a*, lin-7 homolog A (*C. elegans*), *Npr2*, natriuretic peptide receptor 2; *Ccl2*, chemokine (C-C motif) ligand 2; *Cdca3*, cell division cycle associated 3; *Fkbp5*, FK506 binding protein 5; *Gpr64*, G protein-coupled receptor 64; *Inhbb*, inhibin beta-B; *Myc*, myelocytomatosis oncogene; *Ppl*, periplakin.

used two different species models with leptin deficiency, *Lep^{mkyo}/Lep^{mkyo}* rats and *Lep^{ob}/Lep^{ob}* mice.

Some microarray analyses on leptin effects in the liver using *Lep^{ob}/Lep^{ob}* mice have been reported (2, 14, 19). In these studies, leptin was administered daily or continuously and the sampling time point was a few days or more after the beginning of leptin treatment. Under these conditions, the investigators could not separate the secondary effects of chronic metabolic changes, such as body weight reduction and improvement of insulin resistance and dyslipidemia, from the primary effects of leptin. In this study, we sampled livers 6 h after leptin administration under fasting. We confirmed that there was no significant difference in body weight and plasma glucose, insulin and triglyceride concentrations between leptin-treated and saline-treated *Lep^{mkyo}/Lep^{mkyo}* rats and also between leptin-treated and saline-treated *Lep^{ob}/Lep^{ob}* mice. Of course, 6 h

after leptin administration is also the limitation of this study. It might be too early to detect leptin-responsive genes. However, we placed priority on excluding secondary effects. As a result, the profile of leptin-responsive genes in the previous report is quite different from that in the present study. In all these previous reports, expression of metabolism-related genes was detected. On the other hand, in our study, all genes in which we detected change of expression were not known for their relationship with glucose or lipid metabolism in the liver. The genes identified in our study are early responsive ones. Identification of such genes might unveil the mechanism of leptin action that has been unknown so far. The mechanistic study of the genes we have identified here is an issue for the future.

In conclusion, we generated leptin-deficient *Lep^{mkyo}/Lep^{mkyo}* rats by gene-driven ENU mutagenesis. Taking advantage of leptin-treatable *Lep^{mkyo}/Lep^{mkyo}* rats, we compared gene ex-

pressions in the liver not only between *Lep^{mkyo}/Lep^{mkyo}* and WT rats, but also between leptin-treated and saline-treated *Lep^{mkyo}/Lep^{mkyo}* rats, to identify leptin-responsive genes in the liver by microarray analysis. Taking *Lep^{mkyo}/Lep^{mkyo}* rats together with the *Lep^{ob}/Lep^{ob}* mice, we finally identified two leptin-upregulated genes, lin-7 homolog A (*Lin7a*) and natriuretic peptide receptor 2 (*Npr2*), and six leptin-downregulated genes, chemokine (C-C motif) ligand 2 (*Ccl2*), cell division cycle associated 3 (*Cdca3*), FK506 binding protein 5 (*Fkbp5*), inhibin beta B (*Inhbb*), myelocytomatosis oncogene (*C-Myc*), and periplakin (*Ppl*). Although, little is known about the physiological significance of most of these genes in energy metabolism in the liver, the analysis of these genes will bring further understanding of leptin physiology in the future.

ACKNOWLEDGMENTS

We thank Keiko Hayashi for technical assistance. The authors also acknowledge Yoko Koyama for secretarial assistance.

GRANTS

This work was supported by research grants from the Japanese Ministry of Education, Culture, Sports, Science, and Technology, the Japanese Ministry of Health, Labor and Welfare, Uehara Memorial Foundation, Grant-in-aid for Industrial Technology Research Grant Program in 2008 from the New Energy and Industrial Technology Development Organization of Japan (TM:08A02004a), and The European Community's Seventh Framework Programme (FP7/2007-2013) under grant agreement no. HEALTH-F4-2010-241504 (EURATRANS).

DISCLOSURES

No conflicts of interest, financial or otherwise, are declared by the author(s).

AUTHOR CONTRIBUTIONS

Author contributions: M.A.-A., K.E., and K.N. conception and design of research; M.A.-A., K.E., C.E., T.M., A.T., and T.T. performed experiments; M.A.-A. and K.E. analyzed data; M.A.-A., K.E., T.M., T.K., Y.Y., D.A., S.Y.-K., T. Sakai, and K.H. interpreted results of experiments; M.A.-A. prepared figures; M.A.-A. and K.E. drafted manuscript; M.A.-A., K.E., and T. Serikawa edited and revised manuscript; T. Serikawa and K.N. approved final version of manuscript.

REFERENCES

- Campfield LA, Smith FJ, Guisez Y, Devos R, Burn P. Recombinant mouse OB protein: evidence for a peripheral signal linking adiposity and central neural networks. *Science* 269: 546–549, 1995.
- Cohen P, Miyazaki M, Socci ND, Hagge-Greenberg A, Liedtke W, Soukas AA, Sharma R, Hudgins LC, Ntambi JM, Friedman JM. Role for stearoyl-CoA desaturase-1 in leptin-mediated weight loss. *Science* 297: 240–243, 2002.
- Cone RD. The melanocortin-4 receptor. In: *The Melanocortin Receptors*, edited by Cone RD. Totowa, NJ: Humana, 2000, p. 404–445.
- Dubuc PU. The development of obesity, hyperinsulinemia, and hyperglycemia in *ob/ob* mice. *Metabolism* 25: 1567–1574, 1976.
- Ebihara K, Kusakabe T, Hirata M, Masuzaki H, Miyanaga F, Kobayashi N, Tanaka T, Chusho H, Miyazawa T, Hayashi T, Hosoda K, Ogawa Y, DePaoli AM, Fukushima M, Nakao K. Efficacy and safety of leptin-replacement therapy and possible mechanisms of leptin actions in patients with generalized lipodystrophy. *J Clin Endocrinol Metab* 92: 532–541, 2007.
- Ebihara K, Ogawa Y, Masuzaki H, Shintani M, Miyanaga F, Aizawa-Abe M, Hayashi T, Hosoda K, Inoue G, Yoshimasa Y, Gavrilova O, Reitman ML, Nakao K. Transgenic overexpression of leptin rescues insulin resistance and diabetes in a mouse model of lipotrophic diabetes. *Diabetes* 50: 1440–1448, 2001.
- Evans MJ, Kaufman MH. Establishment in culture of pluripotential cells from mouse embryos. *Nature* 292: 154–156, 1981.
- Farooqi IS, Jebb SA, Langmack G, Lawrence E, Cheetham CH, Prentice Hughes IA AM, McCamish MA, O'Rahilly S. Effects of recombinant leptin therapy in a child with congenital leptin deficiency. *N Engl J Med* 341: 879–884, 1999.
- Farooqi IS, Matarese G, Lord GM, Keogh JM, Lawrence E, Agwu C, Sanna V, Jebb SA, Perna F, Fontana S, Lechler RI, DePaoli AM, O'Rahilly S. Beneficial effects of leptin on obesity, T cell hyporesponsiveness, and neuroendocrine/metabolic dysfunction of human congenital leptin deficiency. *J Clin Invest* 110: 1093–103, 2002.
- Hedbacker K, Birsoy K, Wysocki RW, Asilmaz E, Ahima RS, Farooqi IS, Friedman JM. Antidiabetic effects of *IGFBP2*, a leptin-regulated gene. *Cell Metab* 11: 11–22, 2010.
- Hillebrand JJ, Langhans W, Geary N. Validation of computed tomographic estimates of intra-abdominal and subcutaneous adipose tissue in rats and mice. *Obesity* 18: 848–853, 2010.
- Hirabayashi M, Kato M, Aoto T, Ueda M, Hochi S. Rescue of infertile transgenic rat lines by intracytoplasmic injection of cryopreserved round spermatids. *Mol Reprod Dev* 62: 295–299, 2002.
- Kamohara S, Burcelin R, Halaas JL, Friedman JM, Charron MJ. Acute stimulation of glucose metabolism in mice by leptin treatment. *Nature* 389: 374–377, 1997.
- Li X, Wu X, Camacho R, Schwartz GJ, LeRoith D. Intracerebroventricular leptin infusion improves glucose homeostasis in lean type 2 diabetic MKR mice via hepatic vagal and non-vagal mechanisms. *PLoS One* 6: e17058, 2011.
- Liang CP, Tall AR. Transcriptional profiling reveals global defects in energy metabolism, lipoprotein, and bile acid synthesis and transport with reversal by leptin treatment in *ob/ob* mouse liver. *J Biol Chem* 276: 49066–49076, 2001.
- Lord GM, Matarese G, Howard JK, Baker RJ, Bloom SR, Lechler RI. Leptin modulates the T-cell immune response and reverses starvation-induced immunosuppression. *Nature* 394: 897–901, 1998.
- Mashimo T, Yanagihara K, Tokuda S, Voigt B, Takizawa A, Nakajima R, Kato M, Hirabayashi M, Kuramoto T, Serikawa T. An ENU-induced mutant archive for gene targeting in rats. *Nat Gen* 40: 514–515, 2008.
- Ozata M, Ozdemir IC, Licinio J. Human leptin deficiency caused by a missense mutation: multiple endocrine defects, decreased sympathetic tone, and immune system dysfunction indicate new targets for leptin action, greater central than peripheral resistance to the effects of leptin, and spontaneous correction of leptin-mediated defects. *J Clin Endocrinol Metab* 84: 3686–3695, 1999.
- Petersen KF, Oral EA, Dufour S, Befroy D, Ariyan C, Yu C, Cline GW, DePaoli AM, Taylor SI, Gorden P, Shulman GI. Leptin reverses insulin resistance and hepatic steatosis in patients with severe lipodystrophy. *J Clin Invest* 109: 1345–1350, 2002.
- Prieur X, Tung YC, Griffin JL, Farooqi IS, O'Rahilly S, Coll AP. Leptin regulates peripheral lipid metabolism primarily through central effects on food intake. *Endocrinology* 149: 5432–5439, 2008.
- Sharma A, Bartell SM, Baile CA, Chen B, Podolsky RH, McIndoe RA, She JX. Hepatic gene expression profiling reveals key pathways involved in leptin-mediated weight loss in *ob/ob* mice. *PLoS One* 5: e12147, 2010.
- Takaya K, Ogawa Y, Isse N, Okasaki T, Satoh N, Masuzaki H, Mori K, Tamura N, Hosoda K, Nakao K. Molecular cloning of rat leptin receptor isoform complementary DNAs-identification of a missense mutation in Zucker fatty (*fa/fa*) rats. *Biochem Biophys Res Commun* 225: 75–83, 1996.
- Takaya K, Ogawa Y, Hiraoka J, Hosoda K, Yamori Y, Nakao K, Koletsky RJ. Nonsense mutation of leptin receptor in the obese spontaneously hypertensive Koletsky rat. *Nat Genet* 14: 130–131, 1996.
- Tamasi JA, Arey BJ, Bertolini DR, Feyen JH. Characterization of bone structure in leptin receptor-deficient Zucker (*fa/fa*) rats. *J Bone Miner Res* 18: 1605–1611, 2003.
- Tanaka S, Isoda F, Yamakawa T, Ishihara M, Sekihara H. T lymphopenia in genetically obese rats. *Clin Immunol Immunopathol* 86: 219–225, 1998.
- Vaira S, Yang C, McCoy A, Keys K, Xue S, Weinstein EJ, Novack DV, Cui X. Creation and preliminary characterization of a leptin knockout rat. *Endocrinology* 153: 5622–5628, 2012.
- Zhang F, Basinski MB, Beals JM, Briggs SL, Churgay LM, Clawson DK, DiMarchi RD, Furman TC, Hale JE, Hsiung HM, Schoner BE, Smith DP, Zhang XY, Wery JP, Schevitz RW. Crystal structure of the obese protein leptin-E100. *Nature* 387: 206–209, 1997.
- Zhang Y, Proenca R, Maffei M, Barone M, Leopold L, Friedman JM. Positional cloning of the mouse obese gene and its human homologue. *Nature* 372: 425–432, 1994.

In Vitro Characterization and Engraftment of Adipocytes Derived from Human Induced Pluripotent Stem Cells and Embryonic Stem Cells

AU1 ▶

AU2 ▶

Michio Noguchi,¹ Kiminori Hosoda,¹ Maiko Nakane,¹ Eisaku Mori,¹ Kazuhiro Nakao,¹ Daisuke Taura,¹ Yuji Yamamoto,¹ Toru Kusakabe,¹ Masakatsu Sone,¹ Hidetoshi Sakurai,² Junji Fujikura,¹ Ken Ebihara,¹ and Kazuwa Nakao¹

Human induced pluripotent stem (iPS) and embryonic stem (ES) cells can differentiate into a variety of cell types. We reported on adipogenic potential of human iPS and ES cells in vitro. In the present study, we investigate the survival and maintenance of adipocytes differentiated in vitro from human iPS and ES cells after transplantation. Following adipogenic induction in vitro, the differentiated cells exhibited functional properties of adipocytes such as lipid storage, lipolysis, and insulin responsiveness. Subsequently, Matrigel containing the differentiated human iPS and ES cells was transplanted into the subcutaneous tissue of nude mice. After 1–4 weeks, the cells with adipocyte-like features were observed in transplanted Matrigel by histological analysis. The human origin of the cells, their lipid accumulation, and gene expression of adipocyte markers in transplanted cells were then confirmed, suggesting the presence of adipocytes in transplanted Matrigel. When the relative areas of these cells were calculated by dividing the adipocyte areas by the total Matrigel areas, we found that they peaked at 2 weeks after transplantation, and that the adipocytes persisted at 4 weeks. The present study demonstrates that human iPS and ES cells can differentiate into adipocytes with functional properties and that adipocytes derived from human iPS and ES cells can survive and maintain the differentiated properties of adipocytes for at least 4 weeks after transplantation. Adipocytes derived from human iPS and ES cells thus have the potential to open new avenues for stem cell-based research into metabolic diseases and future therapeutic applications.

Introduction

HUMAN INDUCED PLURIPOTENT STEM (iPS) cells exhibit pluripotency in vitro and in vivo like that seen with human embryonic stem (ES) cells [1–3]. Moreover, human iPS cells have been differentiated into a variety of cell types [4–12]. For example, we demonstrated that both human iPS and ES cells have adipogenic potential in vitro [13]. On the other hand, studies involving the transplantation of human iPS cell derivative have been limited to only a few cell types [14–17]. Transplantation studies of derivatives from human PS cells become increasingly important to explore a novel cell therapy for intractable diseases.

Lipodystrophy is a rare syndrome characterized by loss of adipose tissue, which causes insulin resistance, diabetes, dyslipidemia, and ectopic fat accumulation [18,19]. Transplantation of adipose tissue ameliorates the phenotype of lipodystrophy [20]. Further, adipose tissue, adipocytes, and adipose-derived stem cells are therapeutically useful for soft tissue reconstruction after tumor resection [21–24]. Adipocytes derived from human PS cells can be a possible source of

cell therapy for lipodystrophy and soft tissue reconstruction. To date, there have been several reports of using scaffolds to construct adipose-like tissue derived from human adult stem cells and embryonic germ cells [25–28]; however, construction of adipose-like tissue derived from human iPS and ES cells has not been fully demonstrated.

In the present study, we initially assessed functional properties of adipocytes such as lipid storage, lipolysis, and insulin responsiveness in vitro in differentiated human iPS and ES cells. We then studied survival and maintenance of adipocytes derived from human iPS and ES cells following their transplantation.

Materials and Methods

Cell culture

Human iPS cells: 253G4 (G4), 201B7 (B7), and W12, were maintained in a Primate ES medium (ReproCELL) supplemented with 4 ng/mL recombinant human basic fibroblast growth factor (Invitrogen) as we previously described [13]. G4 and B7 were kindly provided by Shinya

¹Department of Medicine and Clinical Science, Kyoto University Graduate School of Medicine, and ²Center for iPS Cell Research and Application (CiRA), Kyoto University, Kyoto, Japan.